

Discovery of ZN-c5, an Orally Bioavailable Selective Estrogen Receptor Degradar (SERD) with Improved Pharmacokinetics

Sayee G. Hegde,* Peter Q. Huang, Kevin D. Bunker, Chad D. Hopkins, Deborah H. Slee, Mehmet Kahraman, Joseph Pinchman, Rakesh K. Sit, Christian C. Lee, Michael Rutgard, Ahmed A. Samatar, Jiali Li, Jianhui Ma, Hooman Izadi, Frank Q. Han, and Alex Chao



Cite This: <https://doi.org/10.1021/acs.jmedchem.5c00887>



Read Online

ACCESS |



Metrics & More

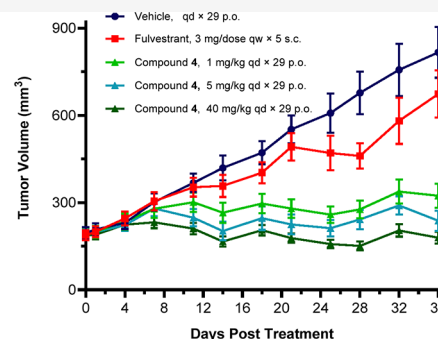
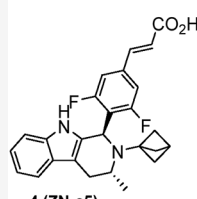


Article Recommendations



Supporting Information

ABSTRACT: Here, we report our strategy to design an optimized oral selective estrogen receptor degrader (SERD), including human pharmacokinetics, by exploiting the bicyclo[1.1.1]pentane (BCP) ring system. The BCP has been shown to serve as a surrogate for phenyl rings and alkyl groups in drug candidates, reducing metabolism and improving physicochemical properties. It has not been extensively profiled in human clinical trials. We optimized a number of molecules and ultimately selected compound **4**, which showed excellent cell potency in breast cancer lines and displayed highly favorable in vitro ADME properties across multiple species. This translated into highly desired exposure in vivo across both rodent and nonrodent species exceeding that observed with other contemporary SERDs and downregulators. After fully profiling the compound, we nominated compound **4** (ZN-c5) for clinical development. Compound **4** advanced into Phase 1/2 clinical trials, which demonstrated high human exposure upon dosing patients with 50 mg once a day.



INTRODUCTION

Breast cancer (BC) is implicated in 12% of global cancer cases, with a significant impact on mortality in women (15% of all cancer-related deaths).¹ Most cases can be classified based on the higher expression levels of the estrogen receptor alpha ($ER\alpha$), without expression of human epidermal growth factor (HER2), namely HR-positive/HER2-negative type breast cancer. Historically, there have been several treatment paradigms often administered sequentially. First, an aromatase inhibitor (AI) to block the biosynthesis of estradiol is used in combination with antihormonal agents. A second strategy employs selective estrogen receptor modulators (SERMs) such as tamoxifen, a mixed agonist/antagonist of the estrogen α - and β - receptors. This approach, while initially effective, can ultimately lead to resistance.² The more recent approach of using a dual ER degrader/antagonist^{3–6} such as the clinically efficacious fulvestrant,⁷ suffers from inherent limitations in delivery.⁸ The compound must be administered via intramuscular (IM) injection which limits the maximum dose to 500 mg/month, and may be the cause of suboptimal receptor occupancy.^{9–11} Therefore, in the past decade, there has been significant interest in the discovery of orally bioavailable small molecule antagonists/degraders, to enable improved systemic exposure leading to enhanced clinical benefit. Several molecules have been evaluated in the clinic and selected examples are depicted in Figure 1. Most SERDs possess either an acrylic acid

or an amine tail group, directed toward helix H12 of the ER α protein that promotes receptor destabilization and degradation by exposing hydrophobic H12 residues. E3 ligase-mediated ubiquitination of K302 and K303 residues in the hinge region of the ER receptor in turn leads to the downstream degradation of the ER protein by the ubiquitin proteasome system.^{12–16} Some examples of SERDs bearing an acrylic acid tail group include GW7604,^{17,18} GDC-0810,¹⁹ AZD9496,²⁰ LSZ102,²¹ D-0502 and G1T48 (Figure 1). Examples of SERDs bearing an amine tail group include SAR439859²² which was halted in 2022, as well as a number of other molecules in late clinical development, including GDC-9545,²³ AZD9833,^{24,25} LY3484356,²⁶ OP-1250²⁷ and the newly approved elacestrant²⁸ (also known as Orserdu). A recent review captures the current molecular landscape.²⁹

RESULTS AND DISCUSSION

Early SERDs and Challenges with Achieving Human Exposure. The discovery of GDC-0810/ARN-810¹⁹ was based

Received: March 31, 2025

Revised: June 10, 2025

Accepted: June 19, 2025

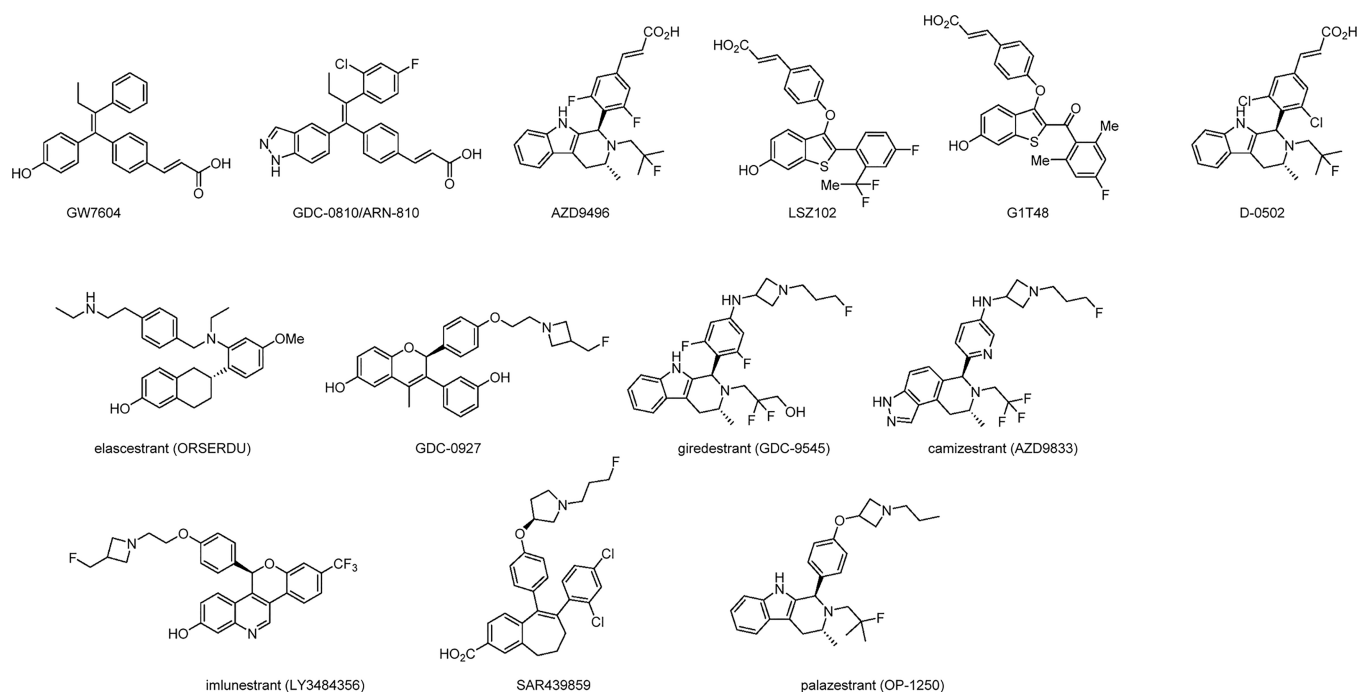


Figure 1. Selected examples of SERDs bearing acrylic acid or amine tails.

on the pioneering work of McDonnell and co-workers (Duke University), Glaxo Wellcome, and later Dupont that led to GW-5638.¹⁷ GDC-0810 showed promise in early clinical trials but ultimately was halted in Phase 2 trials, partly due to the high doses needed for efficacy, adverse events (such as significant GI issues), and associated formulation challenges.³⁰ Meanwhile, AstraZeneca discovered the novel tetrahydrocarboline core²⁰ which was elegantly optimized to AZD9496, a potent antagonist and degrader with high selectivity and good oral exposure across multiple preclinical species, including both rodent and non-rodent. AZD9496 rapidly progressed into Phase 1 clinical studies in ER-positive BC patients as well as a study to assess the pharmacokinetics of different formulations in healthy patients (NCT02780713).³¹ AZD9496 was ultimately replaced by AZD9833 which is currently in Phase 3, likely due to target coverage.^{32,33} Our analysis of AZD9496 identified a few possible metabolic soft spots to explore and optimize, particularly the *N*-isobutyl substituent. In a series of aldosterone synthase inhibitors, the isobutyl functionality was identified as a metabolic soft spot and replacement with an oxetane moiety led to significantly reduced metabolic clearance.^{34,35} We compared the binding poses of AZD9496 and estradiol, an endogenous ligand of ER, in the ER ligand binding domain (LBD) and speculated that alternative lipophilic groups could better occupy the lipophilic pocket defined by Leu525:Leu384 residues.²⁰ Therefore, we considered a handful of replacements, one of which was the bicyclo[1.1.1]pentane (BCP) ring system. The initial synthesis was reported by Wiberg and Connor in 1966.³⁶ More robust synthetic methods have emerged in only the past decade (e.g., see Bunker, Huang and co-workers,³⁷ Baran and co-workers in their seminal early demonstration of the scalability of preparation of BCP amines,^{38,39} and Shire and Anderson for a recent review⁴⁰). The BCP framework represents a nonclassical bioisostere of phenyl rings⁴¹ but also alkynes⁴² and other alkyl groups.⁴³ Pellicciari and co-workers demonstrated how a BCP could be a potent replacement for benzene rings in a new class of glutamate receptor antagonists.⁴⁴ The

pioneering work of Stepan and co-workers at Pfizer illustrated the true potential of the BCP moiety beyond serving as just a spacer.⁴¹ The replacement of a central para-substituted fluorophenyl ring with the BCP ring in the γ -secretase inhibitor BMS-708163 improved passive permeability, solubility, and metabolic stability, resulting in a 4-fold increase in oral exposure in mouse. In vitro and in vivo data were quite compelling, demonstrating that the BCP ring could be utilized to overcome liabilities in drug design and provide the benefits of additional sp³ character to enhance physicochemical and ADME properties.⁴⁵ Multiple groups have recently confirmed the positive benefits on in vivo exposure of the BCP ring.^{46–48} We felt this would be a good opportunity to leverage the BCP moiety to address the less than desired human exposure associated with AZD9496. Furthermore, the goal of our SERD program was to discover and develop a small molecule that could act as both a degrader and a full antagonist of the estrogen receptor and to obviate risks associated with partial agonist activity such as increased risk of endometrial tissue thickening.⁴⁹ This, in combination with a clean safety profile could maximize clinical benefit in patients.

Introduction of Bicyclo[1.1.1]pentyl Group to Fill the Leu525-Leu384 Lipophilic Pocket. A series of compounds were designed and synthesized. Our initial screening cascade focused on testing the ability of synthesized compounds to inhibit the proliferation of the MCF-7 cancer cell line. At the onset we hypothesized that the structural features of the tetrahydrocarboline core would continue to provide selectivity against other nuclear hormone receptor off-targets similar to the exquisitely selective AZD9496.²⁰ Additionally, the cellular readouts would provide an early indication of permeability with the caveat that compounds of interest could also be tested in a separate biochemical binding assay. Select results are shown in Table 1. Based on our analysis of AZD9496 and the potential liability of the isobutyl alkyl side chain, we designed and synthesized compounds 1 and 2 using the Pictet-Spengler cyclization conditions which mostly afforded the *trans* isomer, 138

Table 1. Incorporation of BCP Ring to Occupy the Leu525:Leu384 Lipophilic Pocket

Compound	R ¹	R ²	R ³	MCF-7 ^a IC ₅₀ (nM)	Log D	Cl _{int} ^b (mL/min/kg)	
						mouse	human
AZD9496	H	CH ₃		0.1	2.8	<38	15.9
1	H	CH ₃		ND ^{c,d}	ND ^d	ND ^d	ND ^d
2 ^e	H	CH ₃		42	1.0	<38	<8.6
3	H	CH ₃		1.0	3.3	111	66.7
4 ^e	H	CH ₃		0.3	2.4	<38	<8.6
5	H	CH ₂ CH ₃		11			
6	H	CH ₃		23			
7 ^f	H	CH ₂ CH ₃		75			
8 ^g	CH ₃	CH ₃		43			

^aMCF-7 is a breast cancer cell line. ^bCl_{int} refers to intrinsic microsomal clearance. ^cIC₅₀ in LTED assay: 512 nM. ^dND, not determined. ^eChirality was confirmed by small molecule X-ray or protein-crystallization. ^fIsolated as mixture of isomers. ^gIsolated as mixture of enantiomers.

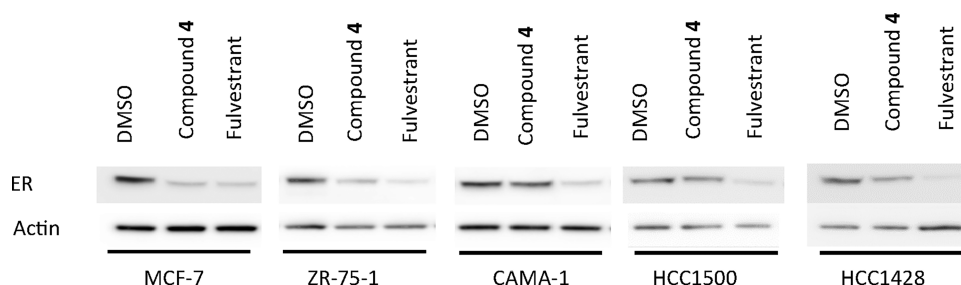


Figure 2. Compound 4 induces ER α degradation in breast cancer cell lines. ER α Western Blot Analysis. Cells were grown in phenol red free DMEM/F12 media supplemented with 8% charcoal-stripped FBS, nonessential amino acids and sodium pyruvate for 48 h before treatment with 100 nM of indicated ligands for 24 h. Immunoblotting performed to determine ER α expression levels using whole cell lysates.

in-line with earlier reports.²⁰ While compound 2 showed modest activity (MCF-7 IC₅₀ = 42 nM), the simpler oxetane exhibited a significant drop in potency (IC₅₀ = 512 nM in an orthogonal, long-term estrogen deprived (LTED) cell assay used earlier in our discovery cascade⁵⁰). In parallel we also began exploring the incorporation of the BCP ring as a lipophilic, compact bioisostere which could occupy the lipophilic pocket. We were gratified when one of our first discoveries, compound 3, showed excellent potency (MCF-7 IC₅₀ = 1 nM). Furthermore, removal of the methylene spacer resulted in compound 4, which was

more potent in the cellular assay (MCF-7 IC₅₀ = 0.3 nM) and bound with high affinity to ER α and ER β (IC₅₀ = 0.4 nM and 0.8 nM, respectively).⁵¹ The enantiomer of compound 4 was not potent (IC₅₀ > 1 μ M, data not shown), consistent with modeling and literature.²⁰ Replacement of the methyl group at R² in compound 4 with an ethyl group (compound 5) resulted in a 37-fold drop in potency (MCF-7 IC₅₀ = 11 nM). To further probe the R³ substituent pocket, we incorporated a sterically bulkier trifluoromethyl-BCP group (compound 6 vs compound 4). We observed a 77-fold drop in cellular potency vs compound 4.

Table 2. Select ADME Properties of Compounds 3 and 4

compound	log D^a	aqueous solubility ^b (μM)	Caco-2 (AB/BA, $10^{-6} \text{ cm s}^{-1}$)	PPB ^c (%)		hERG ^d (μM)
				mouse	human	
3	3.3	434	1.9/1.8	99.9	99.9	>30
4	2.4	6237	8.1/5.7	99.7	99.8	>30

^aLog D was measured in a pH 7.4 buffer. ^bThermodynamic solubility. ^cPlasma protein binding. ^dManual patch clamp assay.

Table 3. Mouse and Rat PK Parameters. Formulation: DMSO/PEG400/150 mM Glycine (pH 9) for IV (5/10/85) and PEG400/PVP/Tween 80/0.5% CMC in Water for PO (9/0.5/0.5/90)

	mouse		rat	
	intravenous	PO (oral)	intravenous	PO (oral)
dose (mg/kg)	3	10	3	10
AUC ($\mu\text{M}\cdot\text{h}$)	26	65	96	283
Cl_{obs} (mL/min/kg)	4.4		1.2	
C_{max} (μM)		10.8		33
$T_{1/2}$ (h)	2.9		4.2	
$V_{\text{d,ss}}$ (L/kg)	1.2		0.48	
F(%) bioavailability		74		88

for AZD9496) and rat (AUC = $283 \mu\text{M}\cdot\text{h}$, F%88 vs AUC = $179 \mu\text{M}\cdot\text{h}$, F%74 for AZD9496). Significantly, the compound was rapidly absorbed (mouse T_{max} = 0.5 h and rat T_{max} = 1 h) and showed a high C_{max} (mouse = $10.8 \mu\text{M}$ and rat = $33 \mu\text{M}$; see Figure 3a,b, respectively, for time-course versus concentration curves). Early in vitro safety profiling was performed to further support development. Compound 4 was tested in human liver microsomes and showed minimal inhibition in a panel of cytochrome P450 enzymes (IC_{50} ranged from 24 to $50 \mu\text{M}$ with the exception of 2C8 (IC_{50} = $0.158 \mu\text{M}$ ⁵⁷), which AZD9496 also significantly inhibited.³² Finally, compound 4 did not inhibit the hERG channel (IC_{50} > $30 \mu\text{M}$).

X-ray Co-Crystal Structure of Compound 4 Complexed with ER α LBD. To further confirm the molecular details of ligand binding, the cocrystal structure of compound 4 with the estrogen receptor LBD was determined to 3.2 Å. Compound 4 occupies the estradiol hormone binding site located toward one end of the ligand binding domain comprised of the N-terminal half of helix-3, the C-terminal half of helix-5, N-terminal end of helix 7, and end of helix 11, with the bicyclo[1.1.1]pentane (BCP) substituted tetrahydrocarboline overlaying nicely with the estradiol steroid core (Figure 4). The indole of compound 4 occupies the same region as the estradiol benzoid ring, and the BCP moiety occupies the same space as the cyclopentyl portion of estradiol.⁵⁸ As in AZD9496,²⁰ the difluorophenyl acrylic acid moiety exits the binding pocket between helices 3 and 11 projecting toward solvent and the disordered helix 11/12 connecting loop, and participates in the previously described unusual acid–acid interaction with the helix 3 Asp351 side chain essential to confer a down regulator-antagonist ligand profile (Figure 5a).²⁰ The crystallography protein construct harbors the previously described L536S engineered mutation in the helix 11/12 interconnecting loop that biases the loop and helix 12 toward an antagonist conformation.⁵⁹

Summary of Key Protein–Ligand Interactions. Several key interactions are evident from the crystal structure of compound 4 in complex with the ligand binding domain of the estrogen receptor α (ER α). Though moderate in resolution, ligand electron density in the compound 4 cocrystal structure is consistent with the assignment as a *trans* (1R,3R) stereoisomer

Similar to that observed with compound 5, replacement of the chiral methyl substituent of compound 3 with an ethyl group or with a *gem*-dimethyl substituent (compounds 7 and 8, both tested as mixtures of isomers) resulted in a significant drop in cellular potency likely reflecting a poorer fit in the LBD of ER and again consistent with literature.²⁰ We further profiled the most potent compounds (3 and 4) in preclinical ADME assays and found that the metabolic stability correlated with lipophilicity (Table 1). Compound 4 showed low intrinsic clearance and well-balanced lipophilicity ($m\text{Cl}_{\text{int}}$ < 38 mL/min/kg and $h\text{Cl}_{\text{int}}$ < 8.6 mL/min/kg, log D = 2.4) compared to the higher turnover associated with the more lipophilic compound 3 ($m\text{Cl}_{\text{int}}$ = 111 mL/min/kg and $h\text{Cl}_{\text{int}}$ = 86.7 mL/min/kg, log D = 3.3). Significantly, compound 4 exhibited much lower human microsomal clearance compared to AZD9496 (Table 1, compound 4: <8.6 mL/min kg vs AZD9496: 15.9 mL/min/kg).

In Vitro Pharmacology Profile of Compound 4. Detailed characterization of the ability of compound 4 to induce ER degradation was performed in breast cancer cell lines MCF-7, ZR-75–1, CAMA-1, HCC1500 and HCC1428 using fulvestrant as a reference with DMSO only as the control vehicle (Figure 2). Compound 4 demonstrated significant degradation of ER, comparable to fulvestrant in several cell lines, and warranted further profiling in the context of an in vivo tumor xenograft model. The poorer activity of compound 4 in both CAMA-1 and HCC1550 has been observed with other acidic side chain-containing SERDs such as AZD9496 and has been attributed to a partial agonist phenotype and/or reduced antiproliferative activity in other cell lines.^{52–55} Compound 4 also did not show any agonist or antagonist activity against other nuclear steroid receptors such as androgen receptor (AR), progesterone receptor (PR), mineralocorticoid receptor (MR) and the glucocorticoid receptor (GR).⁵⁶ Additional mechanistic studies are described in a related publication by Ma, Samatar and co-workers.⁵⁶

Physicochemical, Pharmacokinetic, Drug Metabolism, and Safety Profiling of Compound 4. The physicochemical properties of compound 4 as reflected in cellular permeability and thermodynamic solubility were excellent (Table 2). Efflux ratio was low (0.7) (Caco-2 AB/BA = $8.1/5.7 \times 10^{-6} \text{ cm s}^{-1}$). Compound 3 also showed a relatively low efflux ratio but also much lower P_{app} . Solubility for compound 4 was high (6237 μM). Consistent with the presence of an acrylic acid functionality, both compounds 3 and 4 were highly plasma protein bound (>99.7% in human and mouse plasma, Table 2). The low turnover of compound 4 in mouse and rat microsomal preparations translated to low in vivo IV clearance (mouse: Cl_{obs} = 4.4 mL/min/kg and rat: Cl_{obs} = 1.2 mL/min/kg, dosed at 3 mg/kg) with good $T_{1/2}$ (mouse = 2.9 h and rat = 4.2 h) as shown in Table 3. Upon oral dosing (10 mg/kg) of compound 4 in both mouse and rat, we were gratified to observe the favorable physicochemical properties and metabolic stability were accompanied by excellent exposure and high bioavailability in both mouse (AUC = $65 \mu\text{M}\cdot\text{h}$, F%74 vs AUC = $30 \mu\text{M}\cdot\text{h}$, F%87

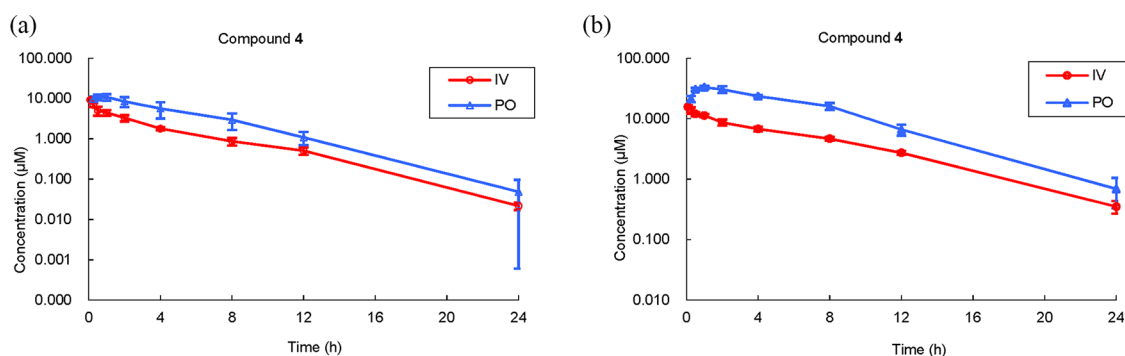


Figure 3. (a) Mouse PK profile of compound 4 (IV: 3 mg/kg, PO: 10 mg/kg). (b) Rat PK profile of compound 4 (IV: 3 mg/kg, PO: 10 mg/kg).

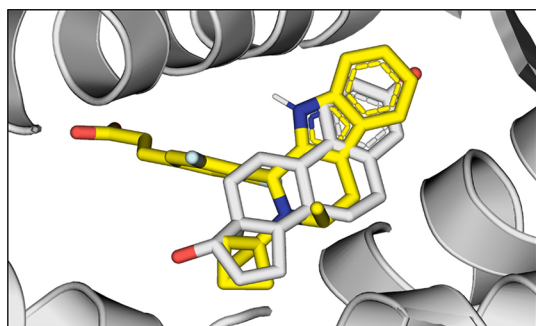


Figure 4. Superposition of compound 4 from the compound 4/ER α LBD co-crystal structure (PDB code 9ECK) with estradiol (PDB 1A52). Ligands are depicted as sticks (compound 4, yellow; estradiol, light gray). Rendering performed with PyMol.⁶⁰

titration was done with parallel arms at 1, 5, and 40 mg/kg, p.o.). Even at 1 mg/kg, compound 4 (MCF-7 cell proliferation inhibition IC_{50} = 0.3 nM) showed significant tumor growth inhibition. Dosing at 5 mg/kg resulted in complete tumor growth inhibition. By comparison, fulvestrant at 3 mg/dose, qw \times 5 gave only 20% tumor growth inhibition. In the WHIM20 xenograft model (Figure 6b), an *ESR1* mutant model (Y537S) without concomitant estrogen supplementation, fulvestrant (200 mg/kg) was compared to a 40 mg/kg dose of compound 4 over 90 days of once-a-day dosing. Compound 4 significantly induced tumor growth inhibition compared to vehicle or fulvestrant and was well-tolerated with no loss in body weight. Additional *in vivo* pharmacology studies with compound 4 are described in more detail in a related publication.⁵⁶

Clinical Candidate Selection. BCP incorporation into the tetrahydrocarboline scaffold afforded active compounds that significantly inhibited tumor growth. Lead compound 4, with the best drug-like properties, demonstrated potency in several cell lines, with significant degradation of ER. Furthermore, compound 4 exhibited excellent exposure and tumor growth inhibition in both endocrine sensitive and mutant ESR mouse xenograft models. The absence of *hERG* signals, no observed *in vitro* cardiotoxicity, manageable CYP450 inhibition, clean profile in the Cerep panel as well as negative results for Ames and micronucleus tests further underscored the favorable safety profile of our lead candidate. Finally, the consistently high bioavailability across multiple preclinical species supported advancement into the clinic. As a point of reference, Figure 7 shows the time course vs concentration curve upon a single dose administration of compound 4 to dogs. Compound 4 shows very low clearance (0.18 mL/min/kg) and high oral bioavailability ($AUC_{0-24\text{ h}} = 2004\text{ }\mu\text{M}\cdot\text{h}$, F%88) (Table 4) with a half-life of 21 h in the IV arm. Taken together with the low predicted human clearance based on liver microsome/hepatocyte studies, and a good safety profile in 28-day GLP toxicity studies, we nominated compound 4 for clinical development.

Human Pharmacokinetics. A Phase 1/2, open label, multicenter trial (NCT03560531) was conducted with compound 4 (later also named ZN-c5) in patients with ER-positive/HER2-negative advanced or metastatic breast cancer. The goal was to assess safety, tolerability, PK, PD, and antitumor activity as a monotherapy as well as in combination with the CDK4/6 inhibitor, palbociclib. The doses began at 50 mg/day and escalated higher using a 28-day cycle.^{51,56} The exposures on Day 1 and Day 15 were 65.7 and 61.3 ($\mu\text{g}\cdot\text{h/mL}$), respectively. Exposures even at this lowest dose exceeded the EC_{100} , the dose (10 mg/kg) which resulted in 100% TGI in the MCF-7-derived xenograft model. The estimated mean elimination half-life

(Figure 5b). Similar to AZD9496, the tetrahydrocarboline core participates in a single hydrogen bond interaction within the hydrophobic binding site by donating a hydrogen from the indole NH to the backbone carbonyl oxygen of Leu-346 (helix-3; 2.2 Å as measured for monomer D) and the indole ring participates in an edge to face T-shaped π - π interaction with Phe-404 of the strand of the β -turn. The core chiral methyl group is retained in compound 4 to maintain the aforementioned potency boost by occupying the 'Phe-404:Phe-425 lipophilic hole' that is occupied by the ethyl group of hydroxytamoxifen²⁰ (Figure 5a). The BCP moiety of compound 4 makes slightly increased van der Waals (VDW) interactions within the Leu525:Leu384 lipophilic hole at one end of the binding site occupied by the cognate 2-fluoro-2-methyl propyl substituent of AZD9496. The BCP and $-\text{CH}_2(\text{CH}_3)_2\text{F}$ moieties occupy 76.5 and 52.1 Å³ of the lipophilic pocket, respectively, in the context of their co-crystal structures (BCP volume occupancy calculated from monomer D). Residues defining this region include Met343, Leu384, Met421, Ile424, Gly521, and Leu525.

In Vivo Efficacy Studies of Compound 4. The advanced lead compound 4 was evaluated in several xenograft mouse models (CDX and PDX models) to first understand how the cellular potency and mouse exposure would translate into an *in vivo* setting relevant for the clinic and second, to set the stage for follow up combination studies. Compound 4 was profiled in a MCF-7 mouse xenograft model (Figure 6a). Day 0 dosing was done in BALB/c nude mice when tumor volumes reached around 200 mm³. Estradiol benzoate pellets were inserted at the beginning of the study to maintain the tumor growth driven by E2. Mice were dosed for 28 days with either vehicle (daily, p.o.), fulvestrant (3 mg/dose qw \times 5, s.c.) or compound 4 (dose

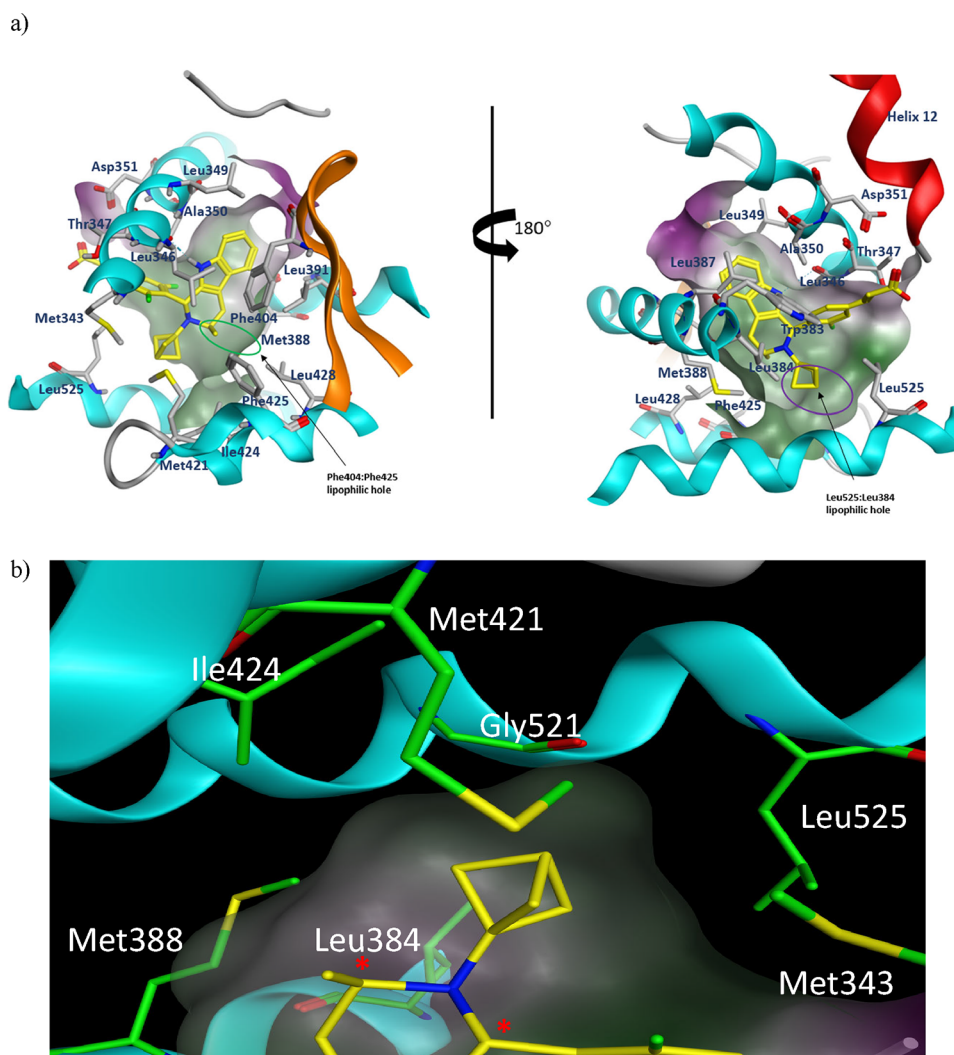


Figure 5. (a) Co-crystal structure of compound 4 complexed with ER α ligand binding domain. Two views of compound 4 bound to ER α ligand binding domain separated by 180° (PDB code 9ECK). The Phe404:Phe425 and Leu525:Leu384 lipophilic holes occupied by the chiral methyl and BCP are highlighted by green and purple ovals, respectively. The molecular surface of the pocket is colored according to its lipophilicity (green: hydrophobic, pink: hydrophilic). Rendering performed with MOE.⁶¹ (b) Close-up view of the compound 4 BCP moiety (PDB code 9ECK) and fit into the Leu525:Leu384 lipophilic hole and other residues within 5 Å that define the subpocket. The 2 chiral centers of the tetrahydropyrido portion of the core are denoted with red asterisks. Rendering performed with MOE.⁶¹

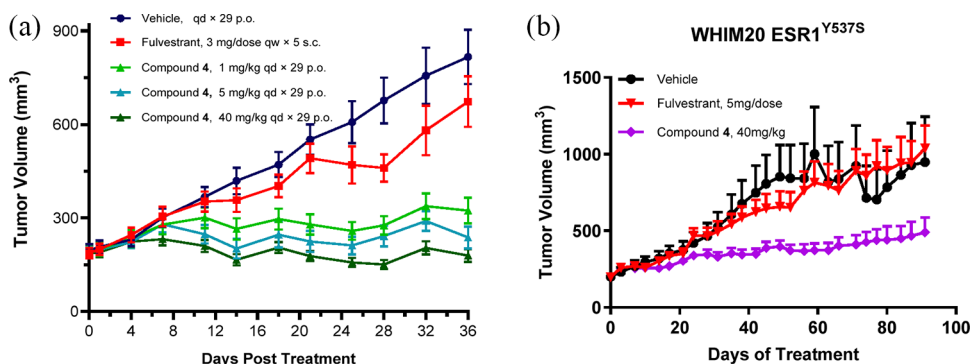


Figure 6. (a) In vivo efficacy of compound 4 in the MCF-7 CDX model. The BALB/c nude mice bearing MCF-7 tumor cells were dosed orally once a day (qd) with compound 4 for 28 days. Fulvestrant was dosed subcutaneously once a week (qw). All the animals in the study received estradiol benzoate injection subcutaneously twice a week. (b) In vivo efficacy of compound 4 in the WHIM20 ESR1^{Y537S} model. The athymic nude mice bearing WHIM20 PDX tumors were orally dosed once a day (qd) with compound 4 (40 mg/kg, qd) for 90 days. Fulvestrant was dosed subcutaneously once a week (qw). In both studies, Compound 4 was formulated in the following vehicle: 20% (2-Hydroxypropyl)- β -cyclodextrin (HP- β -CD) at the proper concentration to dose as indicated. Fulvestrant was formulated in 5% DMSO/95% Kolliphor RH40.

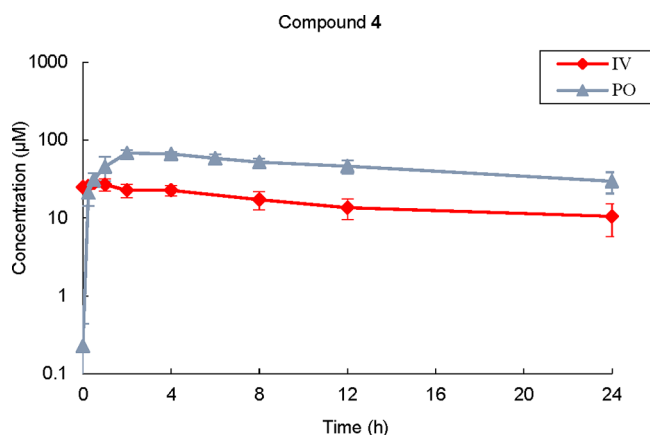


Figure 7. Dog PK profile of compound 4.

Table 4. Dog PK Parameters of Compound 4^a

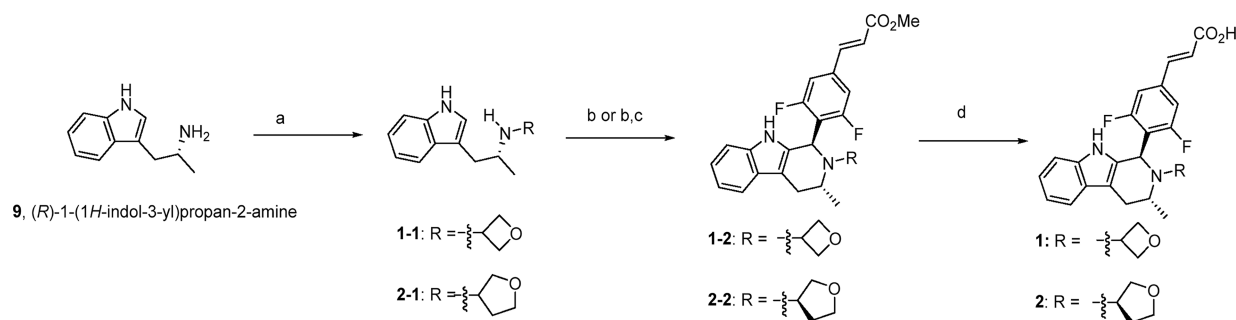
	intravenous	PO (oral)
dose (mg/kg)	3	10
AUC (µM·h)	732	2004
Cl _{obs} (mL/min/kg)	0.18	
C _{max} (µM)		68
T _{1/2} (h)	21	
V _{d,ss} (L/kg)	0.33	
F (%) bioavailability		88

^aCompound 4 was formulated in PEG400/PVP/Tween 80/0.5% CMC in water (9/0.5/0.5/90) for oral dosing and in EtOH/PEG400/30%HPβ-CD (10/40/50) for IV dosing. AUC refers to AUC_{0–24 h}.

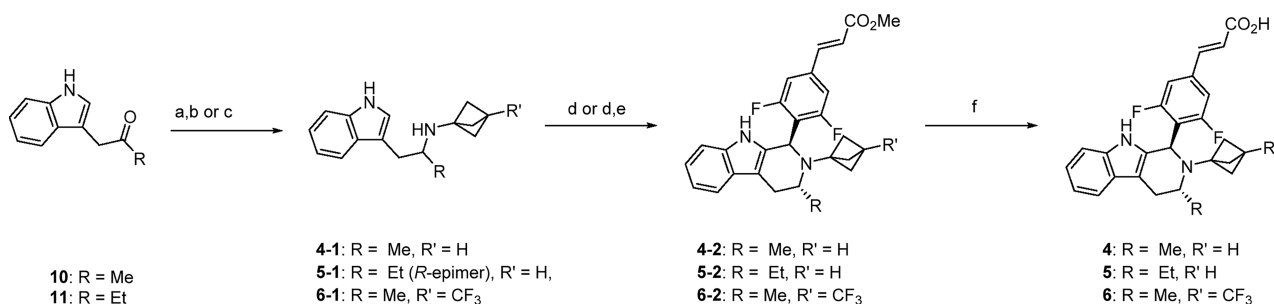
literature.²⁰ Ester hydrolysis under standard conditions using NaOH (aqueous) in MeOH mixtures, gave compounds 1 and 2 (56% yield for both analogs). Purification by chiral, supercritical fluid chromatography (SFC) was used to separate the diastereomers of compound 2. The absolute configuration of compound 2 was verified by single crystal X-ray crystallography. Compounds 4 through 6 were prepared according to Scheme 2. Ketones 10 and 11 were similarly subjected to reductive amination conditions to afford the corresponding amines, 4–1, 5–1 and 6–1. The racemates were typically progressed (without chiral separation unless otherwise indicated) to the subsequent Pictet-Spengler cyclization followed by chiral separation where needed. Similar hydrolysis as in Scheme 1 afforded compounds 4–6 in 26–55% yield. For the methylene homologated *N*-substituted tetrahydrocarbolines shown in Scheme 3, the synthesis entailed reduction of intermediate amides prior to cyclization. The amines 9, 12 and 13 were treated with either T3P or HATU and base in DCM or THF along with bicyclo[1.1.1]pentane-1-carboxylic acid to afford products 3–1, 7–1 and 8–1 in 70–90% yield. Treatment of the amides with lithium aluminum hydride in refluxing THF afforded the corresponding amines 3–2, 7–2 and 8–2. Subsequent Pictet-Spengler cyclization afforded the tetrahydrocarboline esters as mixtures. In the case of 7–3, an unexpected opening of the cyclopropyl ring afforded an ethyl substituted product as confirmed by ¹H NMR (data not shown). The esters were hydrolyzed to the carboxylic acids 3, 7 (mixture of isomers) and 8 (racemic), of which 3 was purified by SFC chiral separation to afford the desired *trans* isomer. Crude products 7 and 8 were purified by rpHPLC to afford final compounds as a mixture of diastereomers or enantiomers, respectively.

CONCLUSIONS

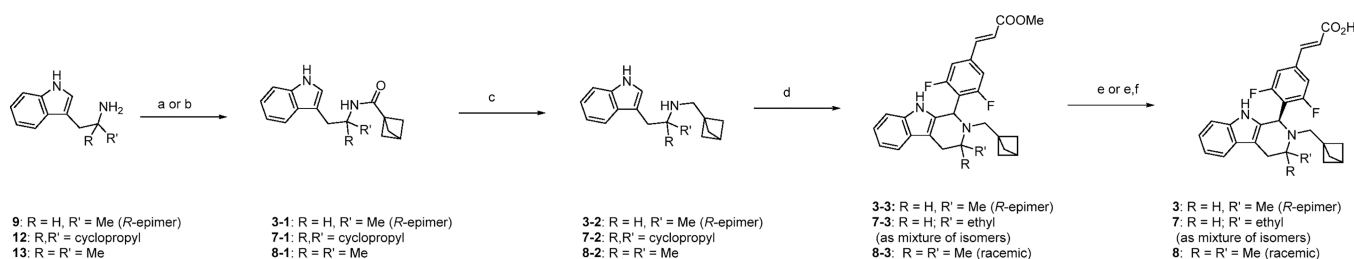
The field of orally bioavailable selective estrogen receptor degraders has expanded greatly over the last 10 years. At the time of initiating our work, the acrylic acid containing clinical compounds suffered from poor human pharmacokinetics despite promising preclinical pharmacokinetics and efficacy. After analyzing the contemporary competitor landscape, we hypothesized that incorporation of the novel BCP ring system could improve the overall profile of SERDs through well-described improved physical properties and enhanced in vitro metabolic stability. This strategy led to a series of BCP-containing SERDs which were potent (including compounds 3 and 4, <1 nM in MCF-7 assay). Optimization of key

Scheme 1. Synthesis of Compounds 1, 2^a

^aReagents and conditions: (a) 9, AcOH, sodium borohydride, MeOH, oxetan-3-one or 3-dihydrofuran-3(2H)-one, 28–40% yield; (b) methyl (E)-3-(3,5-difluoro-4-formylphenyl)acrylate, acetic acid, toluene, 90 °C, 22–32% yield; (c) SFC chiral separation; (d) NaOH (aq) / MeOH, 56% yield.

Scheme 2. Synthesis of Compounds 4–6^a

^aReagents and conditions: (a) **10**, AcOH, NaBH₃CN, MeOH, bicyclo[1.1.1]pentan-1-amine, 58% yield; (b) **11**, AcOH, NaBH₃CN, MeOH, bicyclo[1.1.1]pentan-1-amine, then SFC chiral separation, 33% yield; (c) **10**, AcOH, NaBH₃CN, MeOH, 3-(trifluoromethyl)bicyclo[1.1.1]pentan-1-amine, 47% yield; (d) methyl (*E*)-3-(3,5-difluoro-4-formylphenyl)acrylate, acetic acid, toluene, 90 °C, 9–41% yield; (e) SFC chiral separation; (f) NaOH or LiOH, THF/MeOH, 26–55% yield.

Scheme 3. Synthesis of Compounds 3, 7, 8^a

^aReagents and conditions: (a) **9** or **12**, T3P, DIPEA, THF and bicyclo[1.1.1]pentane-1-carboxylic acid, 70–90% yield; (b) **13**, HATU, DIPEA, DCM and bicyclo[1.1.1]pentane-1-carboxylic acid, 77% yield; (c) LAH, THF, reflux, 41–91% yield; (d) methyl (*E*)-3-(3,5-difluoro-4-formylphenyl)acrylate, acetic acid, toluene, 90 °C, 19–49% yield; (e) NaOH or LiOH, THF/MeOH, 31–41% yield; (f) SFC chiral separation.

392 physicochemical and ADME properties resulted in the clinical
 393 candidate compound **4** (now known as ZN-c5), one of the first
 394 clinical candidates containing a BCP moiety. Compound **4** has
 395 excellent in vivo exposure (mouse AUC = 65 μM·h, rat AUC =
 396 283 μM·h and dog AUC = 2004 μM·h, resulting from a single
 397 dose at 10 mg/kg). More importantly, the human exposure of
 398 ZN-c5 (50 mg qd, AUC = 61.3 (μg·h/mL)) was high,
 399 supporting our initial hypothesis-driven design to utilize a
 400 BCP ring to mitigate metabolism. This resulted in a compound
 401 with higher oral exposure than many of the early clinical
 402 candidates at much lower doses^{63–65} and represents significant
 403 advancement of our understanding of the potential of the BCP
 404 ring in an appropriate design space.

405 ■ EXPERIMENTAL SECTION

406 Starting materials and other reagents were purchased from commercial
 407 suppliers and were used without further purification unless otherwise
 408 indicated. All the reactions were performed under a positive pressure of
 409 nitrogen or argon or with a drying tube, at ambient temperature (unless
 410 otherwise stated), in an anhydrous solvent, unless otherwise indicated.
 411 Analytical thin-layer chromatography (TLC) was performed on glass-
 412 backed silica gel and eluted with the appropriate solvent ratios (v/v).
 413 The reactions were assayed by high-performance liquid chromatog-
 414 raphy (HPLC), LC-MS or TLC and terminated as judged by the
 415 consumption of the starting material. The TLC plates were visualized
 416 by UV, phosphomolybdic acid stain, or iodine stain. Microwave-
 417 assisted reactions were run in a Biotage Initiator. ¹H NMR spectra were
 418 recorded on a Bruker instrument operating at 300 or 400 MHz. ¹H
 419 NMR spectra were obtained as DMSO-*d*₆ or CDCl₃ solutions as
 420 indicated (reported in parts per million, ppm), with chloroform as the
 421 reference standard (7.25 ppm) or DMSO (2.50 ppm). Other NMR
 422 solvents were used as needed. When peak multiplicities are reported,
 423 the following abbreviations are used: s = singlet, d = doublet, t = triplet,

m = multiplet, br = broadened, dd = doublet of doublets, and dt = 424
 doublet of triplets. Coupling constants, when given, are reported in 425
 hertz. The relative stereochemistry was confirmed by 2D-NMR. Mass 426
 spectra were obtained via liquid chromatography–mass spectrometry 427
 (LC–MS) on an Agilent instrument with atmospheric pressure 428
 chemical ionization (APCI) or electrospray ionization (ESI). Reverse 429
 phase HPLC was used to assess purity. All key compounds showed 430
 >95% purity by HPLC except **5** (93.7% purity). Compounds **7** and **8** 431
 were purified to afford mixtures of isomers which were not further 432
 separated. All compounds tested in vivo were at least 95% pure. All the 433
 procedures related to animal handling, care, and the treatment in this 434
 study were performed according to guidelines approved by the 435
 Institutional Animal Care and Use Committee (IACUC) of 436
 Pharmaron, CrownBio or Horizon Biosciences. 437

(R)-N-(1-(1H-indol-3-yl)propan-2-yl)oxetan-3-amine (1–1). 438
 To a stirred solution of (R)-1-(1H-indol-3-yl)propan-2-amine **9** (0.8 439
 g, 4.60 mmol) in ethanol (3 mL) was added oxetane-3-one (0.397 g, 440
 5.52 mmol) and the reaction mixture was stirred at 50 °C for 3 h. The 441
 resulting reaction mixture was cooled to 0 °C, treated with sodium 442
 borohydride (0.262 g, 6.90 mmol) and stirred for 5 h at rt. The mixture 443
 was diluted with ethyl acetate (10 mL) and washed with saturated 444
 aqueous NH₄Cl solution (10 mL). The combined organic layer was 445
 dried over sodium sulfate and concentrated. The crude residue was 446
 purified by column chromatography (SiO₂, 2–3% methanol in DCM) 447
 to afford compound **1–1** (0.3 g, 28% yield) as a colorless, gummy 448
 liquid. ¹H NMR (400 MHz, CDCl₃) δ 8.03 (br s, 1H), 7.58 (d, *J* = 8 Hz, 449
 1H), 7.38 (d, *J* = 8 Hz, 1H), 7.21 (t, *J* = 6.8 Hz, 1H), 7.12 (t, *J* = 6.8 Hz, 450
 1H), 7.07 (d, *J* = 2 Hz, 1H), 4.82–4.77 (m, 1H), 4.71 (d, *J* = 6.8 Hz, 451
 1H), 4.40 (t, *J* = 6.4 Hz, 1H), 4.23 (t, *J* = 6.4 Hz, 1H), 4.13–4.06 (m, 452
 1H), 3.06–3.01 (m, 1H), 2.83 (t, *J* = 6.4 Hz, 2H), 1.09 (d, *J* = 6.4 Hz, 453
 3H); MS (ESI) *m/z* 231.17 [M + H]⁺. 454

Methyl (*E*)-3-(3,5-Difluoro-4-((1*R*,3*R*)-3-methyl-2-(oxetan-3-yl)-2,3,4,9-tetrahydro-1*H*-pyrido[3,4-*b*]indol-1-yl)phenyl)-acrylate (1–2). To a stirred solution of (R)-N-(1-(1H-indol-3-yl)propan-2-yl)oxetan-3-amine **1–1** (0.300 g, 1.30 mmol) in toluene (3 455
 456
 457
 458

459 mL) was added methyl (*E*)-3-(3,5-difluoro-4-formylphenyl)acrylate
460 (0.353 g, 1.56 mmol) and acetic acid (0.156 g, 2.61 mmol). The
461 resulting mixture was stirred at 90 °C for 5 h. The reaction mixture was
462 diluted with EtOAc and washed with water. The combined organic
463 layer was dried over sodium sulfate and concentrated. The residue was
464 purified by reverse phase prep-HPLC to afford compound 1–2 (180
465 mg, 32% yield) as a pale yellow solid. ¹H NMR (300 MHz, DMSO-*d*₆) δ
466 10.6 (br s, 1H), 7.63 (d, *J* = 16.5 Hz, 1H), 7.52 (d, *J* = 10.8 Hz, 2H), 7.40
467 (d, *J* = 7.2 Hz, 1H), 7.19 (d, *J* = 8.4 Hz, 1H), 7.03–6.92 (m, 2H), 6.81
468 (d, *J* = 15.9 Hz, 1H), 5.13 (s, 1H), 4.63 (t, *J* = 6.3 Hz, 1H), 4.51 (t, *J* = 6.9
469 Hz, 1H), 4.20 (t, *J* = 7.2, 1H), 3.97–3.89 (m, 2H), 3.73 (s, 3H), 3.31 (s,
470 1H), 2.93 (dd, *J* = 15 Hz, 4.5 Hz, 1H), 2.57 (d, *J* = 4.5 Hz, 1H), 0.99 (d,
471 *J* = 6.6 Hz, 3H); MS (ESI) *m/z* 439.24 [M + H]⁺.

472 **(*E*)-3-(3,5-Difluoro-4-((1*R*,3*R*)-3-methyl-2-(oxetan-3-yl)-**
473 **2,3,4,9-tetrahydro-1*H*-pyrido[3,4-*b*]indol-1-yl)phenyl)acrylic**
474 **Acid (1).** To a stirred solution of 1–2 (130 mg, 0.296 mmol) in
475 methanol (1.5 mL) was added an aqueous solution of NaOH (35 mg,
476 0.888 mmol, 7.5 M) at 0 °C. The mixture was stirred at rt for 5 h. The
477 reaction mixture was concentrated under reduced pressure to remove
478 methanol. The obtained residue was acidified with 1 N hydrogen
479 chloride solution at 0 °C and then diluted with EtOAc and washed with
480 water. The combined organic layer was dried over sodium sulfate,
481 filtered and concentrated. The residue was triturated with *n*-pentane to
482 afford compound 1 (70 mg, 56% yield) as an off white solid. ¹H NMR
483 (400 MHz, DMSO-*d*₆) δ 12.6 (br s, 1H), 10.6 (br s, 1H), 7.57–7.39
484 (m, 4H), 7.19 (d, *J* = 7.2 Hz, 1H), 7.02–6.93 (m, *J* = 7.2 Hz, 2H), 6.68
485 (d, *J* = 16 Hz, 1H), 5.12 (s, 1H), 4.63 (br s, 1H), 4.52 (br s, 1H), 4.20
486 (br s, 1H), 3.93 (br s, 2H), 2.93 (d, *J* = 15.2 Hz, 1H), 2.56 (br s, 2H),
487 1.00 (br s, 3H); MS (ESI) *m/z* 425.29 [M + H]⁺.

488 ***N*-((*R*)-1-(1*H*-Indol-3-yl)propan-2-yl)tetrahydrofuran-3-**
489 **amine (2–1).** To a stirred solution of compound 9 (0.8 g, 4.60 mmol)
490 in ethanol (3 mL) was added dihydrofuran-3(2*H*) one (0.474 g, 5.52
491 mmol) and acetic acid (0.275 g, 4.60 mmol) at rt and stirred for 3 h. The
492 resulting reaction mixture was cooled to 0 °C and treated with sodium
493 borohydride (0.262 g, 6.90 mmol) and then stirred for 5 h at rt. The
494 mixture was diluted with ethyl acetate (10 mL) and washed with
495 saturated aqueous NH₄Cl solution (10 mL). The combined organic
496 layer was dried over sodium sulfate and concentrated. The obtained
497 residue was purified by column chromatography (SiO₂, 2–3% MeOH/
498 DCM) to afford 2–1 (0.450 g, 40% yield) as a colorless gummy liquid.
499 ¹H NMR (300 MHz, CDCl₃) δ 8.10 (br s, 1H), 7.67–7.55 (m, 1H),
500 7.37 (d, *J* = 8.1 Hz, 1H), 7.20 (t, *J* = 7.2 Hz, 1H), 7.16–7.07 (m, 2H),
501 3.96–3.88 (m, 1H), 3.86–3.52 (m, 3H), 3.28–3.08 (m, 3H), 2.99–
502 2.88 (m, 1H), 2.32–2.17 (m, 1H), 2.17–1.97 (m, 1H), 1.27 (d, *J* = 6.9
503 Hz, 3H); MS (ESI) *m/z* 245.21 [M + H]⁺.

504 **Methyl (*E*)-3-(3,5-Difluoro-4-((1*R*,3*R*)-3-methyl-2-((*R*)-tetra-**
505 **hydrofuran-3-yl)-2,3,4,9-tetrahydro-1*H*-pyrido[3,4-*b*]indol-1-yl)-**
506 **phenyl)acrylate (2–2).** To a stirred solution of 2–1 (0.450 g, 1.84
507 mmol) in toluene (3 mL) was added methyl (*E*)-3-(3,5-difluoro-4-
508 formylphenyl)acrylate (0.501 g, 2.21 mmol) and acetic acid (0.221 g,
509 3.68 mmol). The resulting mixture was stirred at 90 °C for 5 h. The
510 reaction mixture was diluted with EtOAc, washed with water, dried over
511 sodium sulfate, filtered and concentrated. The residue was purified by
512 chiral SFC to afford 2–2 (180 mg, 22% yield) as a pale yellow solid. ¹H
513 NMR (300 MHz, DMSO-*d*₆) δ 10.6 (br s, 1H), 7.62 (d, *J* = 15.9 Hz,
514 1H), 7.50 (d, *J* = 10.5 Hz, 2H), 7.39 (d, *J* = 7.5 Hz, 1H), 7.18 (d, *J* = 8.1
515 Hz, 1H), 7.03–6.92 (m, 2H), 6.79 (d, *J* = 15.9 Hz, 1H), 5.32 (s, 1H),
516 3.85–3.68 (m, 4H), 3.59–3.48 (m, 3H), 3.25 (t, *J* = 7.5 Hz, 1H), 3.08
517 (t, *J* = 7.5 Hz, 1H), 2.89 (dd, *J* = 15 Hz, 4.2 Hz, 1H), 2.55–2.49 (m, 1H),
518 2.24–1.96 (m, 2H), 1.14 (d, *J* = 6.6 Hz, 3H); MS (ESI) *m/z* 453.25 [M
519 + H]⁺. Compound 2–2 elutes as peak 1 and the undesired isomer elutes
520 as peak 2.

521 **(*E*)-3-(3,5-Difluoro-4-((1*R*,3*R*)-3-methyl-2-((*R*)-tetrahydrofuran-**
522 **3-yl)-2,3,4,9-tetrahydro-1*H*-pyrido[3,4-*b*]indol-1-yl)-**
523 **phenyl)acrylic Acid (2).** To a stirred solution of 2–2 (0.180 g, 0.398
524 mmol) in methanol (2 mL) was added an aqueous solution of NaOH
525 (47 mg, 1.19 mmol, 7.5 M) at 0 °C and stirred at rt for 5 h. The reaction
526 mixture was concentrated under reduced pressure to remove solvent.
527 The obtained residue was acidified with 1 N hydrogen chloride solution
528 (aqueous) at 0 °C and extracted with ethyl acetate (3 × 50 mL). The

combined organic layer was dried over Na₂SO₄, filtered and evaporated 529
under reduced pressure to afford the crude product. The residue was 530
purified by chiral SFC to afford 2 (80 mg, 46% yield) as an off white 531
solid. ¹H NMR (300 MHz, DMSO-*d*₆) δ 12.7 (br s, 1H), 10.6 (s, 1H), 532
7.58–7.32 (m, 4H), 7.18 (d, *J* = 8.1 Hz, 1H), 7.02–6.91 (m, 2H), 6.66 533
(d, *J* = 15.6 Hz, 1H), 5.31 (s, 1H), 3.88–3.75 (m, 1H), 3.68–3.48 (m, 534
3H), 3.31–3.22 (m, 1H), 3.08 (t, *J* = 8.1 Hz, 1H), 2.89 (dd, *J* = 15 Hz, 535
3.6 Hz, 1H), 2.54–2.51 (m, 1H), 2.14–1.96 (m, 2H), 1.14 (d, *J* = 6.3 536
Hz, 3H); MS (ESI): *m/z* 439.26 [M + H]⁺; [α]_D = –70.4° (c 0.25, 537
CHCl₃, 24 °C). Single crystal X-ray crystallography was used to assign 538
absolute stereochemistry. 539

540 **(*R*)-*N*-((1-(1*H*-Indol-3-yl)propan-2-yl)bicyclo[1.1.1]pentane-**
541 **1-carboxamide (3–1).** To a stirred solution of (*R*)-1-(1*H*-indol-3-yl) 542
propan-2-amine 9 (0.500 g, 1.14 mmol) in THF (10 mL) was added 543
propylphosphonic anhydride (2.25 mL, 50 wt %/wt in EtOAc) and 544
DIPEA (1.5 mL), at rt. The solution was stirred for 10 min, and then a 545
solution of bicyclo[1.1.1]pentane-1-carboxylic acid (0.375 g, 3.3 546
mmol) was added. The mixture was stirred at rt for an additional 16 547
h. Water (3 mL) was added and the reaction mixture was extracted with 548
EtOAc (2 × 50 mL). The combined organic layers were dried over 549
Na₂SO₄, filtered and evaporated under reduced pressure. The crude 550
product was triturated with ether to obtain 3–1 (700 mg, 90% yield) as 551
a pale yellow solid. MS (ESI) *m/z* 269.26 [M + H]⁺.

552 **(*R*)-*N*-(Bicyclo[1.1.1]pentan-1-ylmethyl)-1-(1*H*-indol-3-yl)-**
553 **propan-2-amine (3–2).** To a stirred solution of 3–1 (700 mg, 2.60 554
mmol) in THF (10 mL) was added LAH (600 mg, 15.8 mmol) in 555
portions at 0 °C. The mixture was heated to reflux for 16 h, cooled to rt 556
and then treated with ice-cold water (50 mL) slowly, and extracted with 557
EtOAc (2 × 50 mL). The combined organic layer was dried over 558
Na₂SO₄, filtered and concentrated under reduced pressure. The crude 559
residue was triturated with ether to obtain crude 3–2 (600 mg, 90% 560
yield) as a pale yellow solid. MS (ESI) *m/z* 255.36 [M + H]⁺.

561 **Methyl (*E*)-3-(4-((1*R*,3*R*)-2-(Bicyclo[1.1.1]pentan-1-ylmethyl)-**
562 **3-methyl-2,3,4,9-tetrahydro-1*H*-pyrido[3,4-*b*]indol-1-yl)-**
563 **3,5-difluorophenyl)acrylate (3–3).** To a stirred solution of crude 564
3–2 (600 mg, 2.35 mmol) in toluene (12 mL), methyl (*E*)-3-(3,5- 565
difluoro-4-formylphenyl)acrylate (540 mg, 2.4 mmol) and acetic acid 566
(285 mg, 4.75 mmol) were added and the mixture was stirred at 90 °C 567
for 12 h. The reaction mixture was neutralized with a saturated, aqueous 568
solution of sodium bicarbonate and extracted with EtOAc (2 × 50 mL). 569
The combined organic layer was dried over Na₂SO₄, filtered and 570
evaporated under reduced pressure to afford crude 3–3 (400 mg, 36% 571
yield) as a mixture of *cis/trans* isomers. MS (ESI) *m/z* 463.38 [M + H]⁺.

572 **(*E*)-3-(4-((1*R*,3*R*)-2-(Bicyclo[1.1.1]pentan-1-ylmethyl)-3-**
573 **methyl-2,3,4,9-tetrahydro-1*H*-pyrido[3,4-*b*]indol-1-yl)-3,5-**
574 **difluorophenyl)acrylic Acid (3).** To a stirred solution of 3–3 (400 575
mg of a mixture of *cis/trans* isomers, 0.86 mmol) in a mixture of THF/
576 MeOH (6 mL, 5:1 v/v) was added aqueous NaOH solution (0.5 mL, 577
1.5 M) at 0 °C and the mixture was stirred at rt for 16 h. Standard 578
aqueous workup and SFC purification afforded 3 (140 mg, 37% yield) 579
as pale yellow solid. ¹H NMR (400 MHz, DMSO-*d*₆) δ 12.50 (br s, 1H), 580
10.50 (s, 1H), 7.55 (d, *J* = 16.0 Hz, 1H), 7.46 (d, *J* = 8 Hz, 2H), 7.39 (d, 581
J = 8 Hz, 1H), 7.16 (d, *J* = 8 Hz, 1H), 6.99 (dd, *J* = 7.6 Hz, 6.8 Hz, 1H), 582
6.94 (dd, *J* = 7.6 Hz, 7.2 Hz, 1H), 6.67 (d, *J* = 16 Hz, 1H), 5.08 (s, 1H), 583
3.45–3.56 (m, 1H), 2.94 (dd, *J* = 12.8 Hz, 4 Hz, 1H), 2.68 (d, *J* = 14 Hz, 584
1H), 2.56 (dd, *J* = 12 Hz, 0.9 Hz, 1H), 2.37 (s, 1H), 2.24 (d, *J* = 14.8 Hz, 585
1H), 1.56 (d, *J* = 8.8 Hz, 3H), 1.46 (d, *J* = 9.2 Hz, 3H), 1.00 (d, *J* = 6.4 586
Hz, 3H); MS (ESI) *m/z* 449.39 [M + H]⁺, [α]_D + 65.6° (c 0.25, MeOH, 587
24 °C).

588 ***N*-(1-(1*H*-Indol-3-yl)propan-2-yl)bicyclo[1.1.1]pentan-1-**
589 **amine (4–1).** To a solution of 1-(1*H*-indol-3-yl)propan-2-one 10 590
(0.062 g, 0.51 mmol) in MeOH (1 mL) was added glacial acetic acid to 591
adjust the pH to 5–6. To this solution was added bicyclo[1.1.1]pentan- 592
1-amine as the hydrochloride salt (0.075 g, 0.43 mmol) followed by 593
sodium cyanoborohydride (0.054 g, 0.86 mmol). The reaction mixture 594
was stirred at room temperature under a nitrogen atmosphere for 16 h. 595
The solvent was removed under reduced pressure, water (5 mL) was 596
added and the mixture was extracted with ethyl acetate (2 × 5 mL). The 597
combined organic layer was washed with saturated sodium bicarbonate 598
solution, brine, dried over sodium sulfate, filtered and concentrated 599

under reduced pressure. The crude residue was purified by flash column chromatography (SiO₂, 3.5% MeOH/DCM) to afford **4–1** (0.060 g, 58% yield) as a light yellow solid. ¹H NMR (400 MHz, CDCl₃) δ 8.03 (s, 1H), 7.64 (d, *J* = 8.0 Hz, 1H), 7.39 (d, *J* = 8.0 Hz, 1H), 7.22 (td, *J* = 8.0, 1.2 Hz, 1H), 7.14 (td, *J* = 8.0, 1.2 Hz, 1H), 7.39 (d, *J* = 2.4 Hz, 1H), 3.21–3.15 (m, 1H), 2.92–2.87 (m, 1H), 2.79–2.74 (m, 1H), 2.36 (s, 1H), 1.86–1.78 (m, 6H), 1.13 (d, *J* = 6.4 Hz, 3H); MS (ESI) *m/z*: 241.26 [*M* + H]⁺.

Methyl (E)-3-(4-((1*R*,3*R*)-2-(Bicyclo[1.1.1]pentan-1-yl)-3-methyl-2,3,4,9-tetrahydro-1*H*-pyrido[3,4-*b*]indol-1-yl)-3,5-difluorophenyl)acrylate (4–2). To a solution of **4–1** (1.3 g, 5.41 mmol) in toluene (15 mL) were added methyl (E)-3-(3,5-difluoro-4-formylphenyl)acrylate (1.2 g, 4.87 mmol) and acetic acid (0.7 mL, 10.8 mmol). The resulting solution was stirred at 80 °C for 2 h. The reaction mixture was cooled to room temperature and poured into a solution of potassium carbonate (20 mL) and extracted with ethyl acetate (3 × 20 mL). The combined organic layer was dried (Na₂SO₄), filtered and concentrated. The crude product was purified by column chromatography (SiO₂, 40% EtOAc/Hexanes) to provide 1.0 g of a racemic mixture of *trans* isomers. The isomers were separated by chiral SFC [Chiralpak AD-H, (250 × 21 mm), 70 mL per min, Liquid CO₂/IPA] to afford **4–2** which elutes as peak 1 (0.381 g, 17% yield) in >99% ee with a retention time of 6.41 min. ¹H NMR (400 MHz, DMSO-*d*₆) δ 10.5 (s, 1H), 7.6 (d, *J* = 16.0 Hz, 1H), 7.5 (d, *J* = 10.0 Hz, 2H), 7.4 (d, *J* = 7.6 Hz, 1H), 7.2 (d, *J* = 7.6 Hz, 1H), 7.0 (m, 2H), 6.8 (d, *J* = 16.0 Hz, 1H), 5.3 (s, 1H), 3.7 (s, 3H), 3.6 (m, 1H), 2.9 (m, 1H), 2.6 (m, 1H), 2.3 (s, 1H), 1.7 (d, *J* = 8.0 Hz, 3H), 1.6 (d, *J* = 1.2 Hz, 3H), 1.2 (d, *J* = 6.4 Hz, 3H); LC-MS *m/z*: 449.6 [*M* + H]. The undesired enantiomer elutes as Peak 2 (9.59 min).

(E)-3-(4-((1*R*,3*R*)-2-(Bicyclo[1.1.1]pentan-1-yl)-3-methyl-2,3,4,9-tetrahydro-1*H*-pyrido[3,4-*b*]indol-1-yl)-3,5-difluorophenyl)acrylic Acid (4). To a solution of **4–2** (0.381 g, 0.850 mmol) in THF (4 mL) and MeOH (2 mL) was added an aqueous sodium hydroxide solution (1.2 mL, 7.5 M). The solution was stirred at room temperature for 4 h. Water (10 mL) was added to the reaction mixture and the pH of aqueous solution was adjusted to 5 by addition of 2 N HCl solution. The solution was extracted with diethyl ether (3 × 50 mL). The combined organic layer was dried over sodium sulfate, filtered and concentrated under reduced pressure. The crude product was purified by reverse phase prep HPLC [PURITAS PREP C₁₈ (250 × 21.2 mm), 17 mL/min, (3 mM ammonium acetate + 0.02% formic acid) in water/acetonitrile, retention time 4.47 min] to afford **4** (0.110 g, 29% yield) as a pale yellow solid. ¹H NMR (400 MHz, DMSO-*d*₆) δ 12.4 (s, 1H), 10.5 (s, 1H), 7.6 (d, *J* = 16.0 Hz, 1H), 7.5 (d, *J* = 10.0 Hz, 2H), 7.4 (d, *J* = 8.0 Hz, 1H), 7.2 (d, *J* = 7.6 Hz, 1H), 6.9 (m, 2H), 6.7 (d, *J* = 16.0 Hz, 1H), 5.3 (s, 1H), 3.6 (m, 1H), 2.9 (m, 1H), 2.6 (m, 1H), 2.3 (s, 1H), 1.8 (d, *J* = 8.4 Hz, 3H), 1.6 (d, *J* = 1.2 Hz, 3H), 1.2 (m, 3H); MS (ESI) *m/z*: 435.4 [*M* + H]⁺.

N-(1-(1*H*-Indol-3-yl)butan-2-yl)bicyclo[1.1.1]pentan-1-amine (5–1). To a stirred solution of bicyclo[1.1.1]pentan-1-amine HCl salt (0.9 g, 7.69 mmol), in MeOH (180 mL) was added AcOH to adjust its pH to 5–6. Compound **11** (1.2 g, 6.41 mmol) was added at rt, followed by NaCNBH₃ (720 mg, 11.5 mmol) and the mixture was stirred for 12 h at rt under argon atmosphere. Solvent was removed in vacuo and the resultant residue was poured into water and extracted with EtOAc (2 × 100 mL). The combined organic layers were washed with aq NaHCO₃, water, brine, dried over sodium sulfate, filtered and concentrated under reduced pressure. The resultant residue was first purified by column chromatography (3:7 ethyl acetate in hexanes) to afford *N*-(1-(1*H*-indol-3-yl)butan-2-yl)bicyclo[1.1.1]pentan-1-amine (0.90 g, 56% yield) as a yellow liquid. The enantiomers were further purified by SFC chromatography [Lux Cellulose-2, 15% (0.5% DEA in MeOH)] to afford peak 1 (0.160 g, 32.0% yield) in >99% ee and the desired peak 2 (0.160 g, 33.0% yield) in >99% ee. MS (ESI) *m/z* 255.0 [*M* + H]⁺.

(E)-Methyl 3-(4-((1*R*,3*R*)-2-(Bicyclo[1.1.1]pentan-1-yl)-3-ethyl-2,3,4,9-tetrahydro-1*H*-pyrido[3,4-*b*]indol-1-yl)-3,5-difluorophenyl)acrylate (5–2). To a stirred solution of **5–1** (160 mg, 0.63 mmol) in toluene (8.0 mL) were added (E)-methyl-3-(3,5-difluoro-4-formylphenyl) acrylate (142.0 mg, 0.63 mmol) followed by

AcOH (0.75 mL, 1.26 mmol) and stirred at 90 °C for 6 h. The reaction mixture was allowed to warm to room temperature, diluted with water and extracted with ethyl acetate. The combined organic layers were dried over Na₂SO₄, filtered and concentrated. The resultant residue was purified by column chromatography (SiO₂, 2:8 ethyl acetate in hexanes) to afford **5–2** (80 mg, 27% yield). MS (ESI) *m/z* 463.7 [*M* + H]⁺.

(E)-3-(4-((1*R*,3*R*)-2-(Bicyclo[1.1.1]pentan-1-yl)-3-ethyl-2,3,4,9-tetrahydro-1*H*-pyrido[3,4-*b*]indol-1-yl)-3,5-difluorophenyl)acrylic Acid (5). To a stirred solution of **5–2** (80 mg, 0.17 mmol) in THF/water (5.0 mL, 1:1) was added LiOH (42 mg, 1.03 mmol) at 0 °C and the mixture was stirred at rt for 6 h. The reaction mixture was washed with diethyl ether and the separated aqueous layer was acidified to pH 3–4 with 1.0 M HCl solution at 0 °C. The resulting solid was filtered, washed with water and dried to afford **5** (0.011 g, 14% yield) as a pale yellow solid. ¹H NMR (300 MHz, DMSO-*d*₆) δ 12.56 (br s, 1H), 10.62 (br s, 1H), 7.56–7.40 (m, 4H), 7.18 (d, *J* = 5.7 Hz, 1H), 7.00–6.92 (m, 2H), 6.66 (d, *J* = 11.7 Hz, 1H), 5.39 (s, 1H), 3.18 (s, 1H), 2.77 (s, 2H), 2.25 (s, 1H), 1.77–1.63 (m, 6H), 1.43 (s, 1H), 1.23 (s, 1H), 0.85 (m, 3H); MS (ESI) *m/z* 449.11 [*M* + H]⁺, [α]_D²⁵ – 279.1 (c 0.5, MeOH).

N-(1-(1*H*-Indol-3-yl)propan-2-yl)-3-(trifluoromethyl)bicyclo[1.1.1]pentan-1-amine (6–1). To a stirred solution of 1-(1*H*-indol-3-yl)propan-2-one (0.400 g, 2.31 mmol) in methanol (3 mL) was added 3-(trifluoromethyl)bicyclo[1.1.1]pentan-1-amine (0.518 g, 2.77 mmol) and acetic acid (14 mg, 0.231 mmol) and the mixture was stirred at rt for 16 h. The resulting solution was cooled to 0 °C and sodium cyanoborohydride (0.290 g, 4.62 mmol) was added followed by additional stirring for 5 h at rt. The reaction was diluted with ethyl acetate (10 mL) and washed with saturated, aqueous NH₄Cl solution (10 mL). The combined organic layer was dried over sodium sulfate, filtered and concentrated. The crude residue was purified by column chromatography using (SiO₂, 15% EtOAc/Hexane) to afford 0.4 g of *N*-(1-(1*H*-indol-3-yl)propan-2-yl)-3-(trifluoromethyl)bicyclo[1.1.1]pentan-1-amine (**6–1**) which was used without further purification. MS (ESI) *m/z*: 309.18 [*M* + H]⁺.

Methyl (E)-3-(3,5-Difluoro-4-((1*R*,3*R*)-3-methyl-2-(3-(trifluoromethyl)bicyclo[1.1.1]pentan-1-yl)-2,3,4,9-tetrahydro-1*H*-pyrido[3,4-*b*]indol-1-yl)phenyl)acrylate (6–2). To a stirred solution of **6–1** (1.2 g, 3.90 mmol) in toluene (6 mL) was added methyl (E)-3-(3,5-difluoro-4-formylphenyl)acrylate (0.880 g, 3.90 mmol) and acetic acid (0.467 g, 7.79 mmol). The resulting mixture was stirred at 90 °C for 5 h. The reaction mixture was diluted with EtOAc and washed with water. The combined organic phase was dried over sodium sulfate, filtered and concentrated. The residue was purified by chiral SFC (Chiralcel OD-H (5 μm, 250 × 21 mm) %CO₂: 85.0%, % Cosolvent (EtOH): 15.0%, to afford 180 mg (9% yield) of **6–2**. ¹H NMR (300 MHz, DMSO-*d*₆) δ 10.6 (br s, 1H), 7.74–7.52 (m, 3H), 7.41 (d, *J* = 6.6 Hz, 1H), 7.18 (d, *J* = 6.9 Hz, 1H), 7.02–6.92 (m, 2H), 6.82 (d, *J* = 15.9 Hz, 1H), 5.36 (s, 1H), 3.75 (s, 3H), 3.61 (br s, 1H), 3.01–2.95 (m, 1H), 2.63–2.58 (m, 1H), 2.01 (d, *J* = 9.3 Hz, 3H) 1.83 (d, *J* = 9.3 Hz, 3H), 1.09 (d, *J* = 6.6 Hz, 3H); MS (ESI) *m/z* 517.18 [*M* + H]⁺. Compound **6–2** elutes as peak 1 and the undesired enantiomer elutes as peak 2.

(E)-3-(3,5-Difluoro-4-((1*R*,3*R*)-3-methyl-2-(3-(trifluoromethyl)bicyclo[1.1.1]pentan-1-yl)-2,3,4,9-tetrahydro-1*H*-pyrido[3,4-*b*]indol-1-yl)phenyl)acrylic Acid (6). To a stirred solution of **6–2** (180 mg, 0.349 mmol) in methanol (1.5 mL) was added aqueous solution of NaOH (0.13 mL, 0.039 g, 0.988 mmol, 7.5 M) solution at 0 °C and the mixture was stirred at rt for 5 h. The reaction mixture was concentrated under reduced pressure to remove methanol. The residue was acidified with 1 N HCl solution at 0 °C, diluted with EtOAc and washed with water. The combined organic layer was dried over sodium sulfate, filtered and concentrated. The crude residue was purified by SFC (Chiralcel OJ-H (5 μm, 250 × 21 mm); %CO₂: 50.0%; % Cosolvent (EtOH): 50.0%, to afford **6** (90 mg, 55% yield) as an off white solid. ¹H NMR (300 MHz, DMSO-*d*₆) δ 10.6 (br s, 1H), 7.62–7.39 (m, 4H), 7.18 (d, *J* = 7.5 Hz, 1H), 7.03–6.92 (m, *J* = 7.2 Hz, 2H), 6.68 (d, *J* = 16.2 Hz, 1H), 5.38 (s, 1H), 3.62 (br s, 1H), 3.05–2.97 (m, 1H), 2.63–2.58 (m, 1H), 2.08–1.79 (m, 6H), 1.09 (d, *J*

738 = 6 Hz, 3H); MS (ESI) m/z 503.26 $[M + H]^+$, $[\alpha]_D = -58.4^\circ$ (c 0.25, 739 $CHCl_3$, 24 $^\circ C$).

740 ***N*-(1-((1*H*-Indol-3-yl)methyl)cyclopropyl)bicyclo[1.1.1]-**
741 **pentane-1-carboxamide (7-1).** To a stirred solution of 12 (0.19 g,
742 1.02 mmol) in dichloromethane (3.92 mL) was added HATU (0.312 g,
743 1.326 mmol) and *N,N*-Diisopropylethylamine (0.36 mL, 2.04 mmol) at
744 rt and the mixture was stirred for 10 min. Bicyclo[1.1.1]pentane-1-
745 carboxylic acid (0.13 g, 1.11 mmol) was added and the mixture was
746 stirred at rt for 16 h. Ethyl acetate (15 mL) was added and the organic
747 phase was washed with saturated, aqueous sodium bicarbonate
748 solution. The organic layer was separated, dried over sodium sulfate,
749 filtered and concentrated. The resulting residue was purified by flash
750 chromatography (SiO_2 , 30–60% EtOAc in hexane) to afford 7-1 (0.20
751 g, 70% yield) as an off-white solid. MS (APCI) m/z 281.16 $[M + H]^+$.

752 **1-((1*H*-Indol-3-yl)methyl)-*N*-(bicyclo[1.1.1]pentan-1-ylmethyl)cyclopropanamine (7-2).** To a stirred solution of 7-1
753 (0.20 g, 0.71 mmol) in THF (2.85 mL) was added LAH (1.78 mL, 2 M
754 LAH in THF solution, 3.57 mmol) dropwise at 0 $^\circ C$ and the mixture
755 was refluxed for 18 h. The reaction mixture was quenched sequentially
756 with cold (0–5 $^\circ C$) water (0.15 mL), an aqueous solution of 15%
757 NaOH (0.30 mL) and water (0.50 mL). The resulting mixture was
758 extracted with EtOAc (3 \times 10 mL). The separated organic phase was
759 dried over sodium sulfate, filtered and concentrated. The resulting
760 residue was purified by flash chromatography (SiO_2 , 0–50% (9:1
761 DCM:MeOH with ammonia) in DCM to afford 7-2 (0.13 g, 68%
762 yield) as a white solid. MS (APCI) m/z 267.18 $[M + H]^+$.

764 **Methyl (E)-3-(4-(2-(Bicyclo[1.1.1]pentan-1-ylmethyl)-3-ethyl-2,3,4,9-tetrahydro-1*H*-pyrido[3,4-*b*]indol-1-yl)-3,5-difluorophenyl)acrylate (7-3).** To a stirred solution of 7-2 (0.11,
765 0.41 mmol) in toluene were added (*E*)-ethyl 3-(3,5-difluoro-4-
766 formylphenyl)acrylate (0.11 g, 0.11 mmol) and acetic acid (0.050 g,
767 0.83 mmol) and stirred at 80 $^\circ C$ for 3 h. The crude reaction products
768 suggested that the cyclopropyl ring had been cleaved. The reaction
769 mixture was diluted with EtOAc and washed with water. The organic
770 layer was separated, dried over sodium sulfate and concentrated. The
771 resulting residue was purified by flash chromatography (SiO_2 , 0–20%
772 EtOAc in hexane) to afford 7-3 (0.10 g, 49% yield) as a yellow solid.
773 MS (APCI) m/z 491.24 $[M + H]^+$.

776 **(E)-3-(4-(2-(Bicyclo[1.1.1]pentan-1-ylmethyl)-3-ethyl-2,3,4,9-tetrahydro-1*H*-pyrido[3,4-*b*]indol-1-yl)-3,5-difluorophenyl)acrylic Acid (7).** To a stirred solution of 7-3 (0.10 g,
777 0.20 mmol) in a mixture of methanol (1 mL), THF (1 mL) and water (1
778 mL) was added sodium hydroxide (0.024 g, 0.61 mmol) at 0 $^\circ C$ and
779 stirred at rt for 2 h until starting material was completely consumed.
780 The mixture was concentrated under reduced pressure and the residue
781 was acidified to pH of 4 using aqueous citric acid solution (1 M) at 0 $^\circ C$.
782 The resulting precipitate was extracted with EtOAc and concentrated.
783 The solid was dissolved in DMSO (1.5 mL) and purified by reverse-
784 phase HPLC chromatography using 10–50% acetonitrile (contains
785 0.15% formic acid) in water (contains 0.1% formic acid) to afford 7
786 (0.03 g, 31% yield) as a mixture of isomers which were not further
787 purified. 1H NMR (400 MHz, DMSO- d_6) δ 12.51 (s, 1H), 10.57 (s,
788 1H), 7.54 (d, J = 16.0 Hz, 1H), 7.45 (d, J = 12 Hz, 2H), 7.41 (d, J = 7.8
789 Hz, 1H), 7.18 (d, J = 7.8 Hz, 1H), 7.03–6.91 (m, 2H), 6.67 (d, J = 16.0
790 Hz, 1H), 5.15 (s, 1H), 3.00 (qd, J = 4.6, 8.9 Hz, 1H), 2.81–2.62 (m,
791 3H), 2.40 (s, 1H), 2.29 (br d, J = 14.4 Hz, 1H), 1.64–1.50 (m, 7H),
792 1.36–1.21 (m, 1H), 0.84 (t, J = 7.3 Hz, 3H); MS (APCI) m/z 463.21
793 $[M + H]^+$.

796 ***N*-(1-((1*H*-Indol-3-yl)-2-methylpropan-2-yl)bicyclo[1.1.1]-**
797 **pentane-1-carboxamide (8-1).** To a stirred solution of 13 (0.31 g,
798 1.65 mmol) in dichloromethane (6.33 mL) were added HATU (0.50 g,
799 2.14 mmol) and *N,N*-Diisopropylethylamine (0.57 mL, 3.29 mmol) at
800 rt and stirred for 10 min. Bicyclo[1.1.1]pentane-1-carboxylic acid (0.20
801 g, 1.81 mmol) was added and the mixture was stirred at rt for 16 h. The
802 reaction mixture was diluted with EtOAc (15 mL) and washed with
803 saturated sodium bicarbonate (aqueous) solution. The organic layer
804 was separated, dried over sodium sulfate, filtered and concentrated. The
805 resulting residue was purified by flash chromatography (SiO_2 , 30–60%
806 EtOAc in hexane) to afford 8-1 (0.36 g, 77% yield). MS (APCI) m/z
807 283.17 $[M + H]^+$.

***N*-(Bicyclo[1.1.1]pentan-1-ylmethyl)-1-((1*H*-indol-3-yl)-2-**
808 **methylpropan-2-amine (8-2).** To a stirred solution of 8-1 (0.36 g,
809 1.28 mmol) in THF was added LAH (5.19 mL, 2 M LAH in THF, 10.38
810 mmol) dropwise at 0 $^\circ C$ and the mixture was refluxed for 18 h. The
811 reaction mixture was quenched sequentially with cold (0–5 $^\circ C$) water
812 (0.40 mL) slowly, then an aqueous solution of 15% NaOH (0.80 mL)
813 and water (1.2 mL). The resulting mixture was extracted with EtOAc (2
814 \times 20 mL). The separated organic phase was dried over sodium sulfate,
815 filtered, and concentrated under reduced pressure. The resulting
816 residue was purified by flash chromatography (SiO_2 , 0–50% (9:1
817 DCM:MeOH with ammonia) in DCM to afford 8-2 (0.14 g, 41%
818 yield). MS (APCI) m/z 269.19 $[M + H]^+$.

820 **Methyl (E)-3-(4-(2-(Bicyclo[1.1.1]pentan-1-ylmethyl)-3,3-di-**
821 **methyl-2,3,4,9-tetrahydro-1*H*-pyrido[3,4-*b*]indol-1-yl)-3,5-**
822 **difluorophenyl)acrylate (8-3).** To a stirred solution of 8-2 (0.07 g,
823 0.26 mmol) in toluene (0.65 mL) was added (*E*)-ethyl 3-(3,5-difluoro-
824 4-formylphenyl)acrylate (0.069 g, 0.29 mmol) and acetic acid (0.031 g,
825 0.52 mmol) and stirred at 90 $^\circ C$ for 5 h. The reaction mixture was
826 diluted with EtOAc and washed with water. The separated organic
827 phase was dried over sodium sulfate, filtered and concentrated. The
828 resulting residue was purified by flash chromatography (SiO_2 , 0–15%
829 ethyl acetate in hexane) to afford 8-3 (0.025 g, 19% yield) as a pale
830 yellow solid. MS (APCI) m/z 491.24 $[M + H]^+$.

831 **(E)-3-(4-(2-(Bicyclo[1.1.1]pentan-1-ylmethyl)-3,3-dimethyl-**
832 **2,3,4,9-tetrahydro-1*H*-pyrido[3,4-*b*]indol-1-yl)-3,5-**
833 **difluorophenyl)acrylic Acid (8).** To a stirred solution of 8-3 (0.02 g,
834 0.041 mmol) in a mixture of methanol (1 mL), THF (1 mL) and water
835 (1 mL) was added sodium hydroxide (4.8 mg, 0.12 mmol) at 0 $^\circ C$ and
836 stirred at rt for 2 h. The mixture was concentrated under reduced
837 pressure and the residue was acidified with an aqueous solution of citric
838 acid (1 M) at 0 $^\circ C$ to adjust pH to 4. The precipitate was extracted with
839 EtOAc and concentrated. The resulting residue was dissolved in DMSO
840 (1 mL) and purified by reversed-phase HPLC column chromatography
841 using 10–60% acetonitrile (contains 0.1% formic acid) in water
842 (contains 0.1% formic acid) to obtain 8 (0.008 g, 41% yield) as a
843 mixture of enantiomers which were not further purified. 1H NMR (400
844 MHz, $CDCl_3$) δ 7.62 (br d, J = 16.0 Hz, 1H), 7.53–7.45 (m, 1H), 7.22–
845 7.18 (m, 1H), 7.14–7.08 (m, 2H), 7.03 (d, J = 8 Hz, 2H), 6.43 (d, J =
846 16.0 Hz, 1H), 5.14 (br s, 1H), 3.02 (br d, J = 16.4 Hz, 1H), 2.91 (br d, J =
847 13.9 Hz, 1H), 2.63 (br d, J = 14.9 Hz, 1H), 2.28 (br d, J = 16.4 Hz,
848 1H), 2.19 (s, 1H), 1.33–1.22 (m, 6H), 1.18 (br d, J = 8 Hz, 3H), 1.03
849 (s, 3H) (missing carboxylic acid and NH protons); MS (APCI) m/z
850 463.21 $[M + H]^+$.

851 **Construct Generation.** The ESR1 gene (UniProt P03372) encoding
852 amino acid residues 298–553 of the ligand binding domain was codon
853 optimized, synthesized (Integrated DNA Technologies), cloned into
854 the pET28a vector, which contains a TEV protease cleavable N-
855 terminal 6xHis fusion tag. Three engineered amino acid mutations
856 corresponding to C381S, C417S, and L536S were incorporated into the
857 DNA construct compared to the ESR1 protein sequence.

858 **Protein Expression and Purification.** The plasmid expression
859 construct was transformed and expressed in *E. coli* BL21 Rosetta
860 (DE3) cells in TB media with IPTG induction (0.2 mM) at an OD600
861 at 1.0. Cultures were incubated at 17 $^\circ C$ postinduction and harvested
862 via centrifugation overnight. Cells were resuspended in lysis buffer (25
863 mM tris, pH 8.0, 500 mM NaCl, 10 mM imidazole, 10% glycerol, 1 mM
864 PMSF, 1 mM Benzamidine, 5 mM beta-mercaptoethanol) before
865 sonication and clarification via high-speed centrifugation at 13 krpm.
866 The supernatant was applied using a AKTA Purifier FPLC to HisTrap
867 HP columns (GE Healthcare), before the columns were washed with
868 lysis buffer supplemented with increasing imidazole concentrations (up
869 to 40 mM) and the bound protein was eluted with lysis buffer
870 supplemented with 250 mM imidazole. Following overnight dialysis,
871 the ER α -LBD protein was incubated with TEV at room temperature for
872 4 h. Cleaved ER α -LBD was passed through Ni-NTA beads and collected
873 in the flowthrough. Gel filtration using a Superdex 75 10/300 column
874 pre-equilibrated with 25 mM tris, pH 8.0, 500 mM NaCl, 10% glycerol,
875 5 mM beta-mercaptoethanol on AKTA Purifier FPLC was performed
876 to further purify the protein. The final protein for crystallization trials

was concentrated to 1 mg/mL and flash frozen in liquid nitrogen in aliquots then stored at -80°C .

Protein Co-Crystallization and Harvesting. Initially, the compound 4 was added to purified protein at 1 mg/mL to a final concentration of 0.2 mM from a 40 mM DMSO stock and incubated for 30 min at 4°C before concentration of the protein to ~ 10 mg/mL. The protein was subjected to extensive crystallization trials using commercially available screens as well as literature ER α -LBD crystallization conditions to identify initial crystallization conditions. Initial crystals appeared in 0.1 M tris pH 8.0, 20% PEG 3350, 200 mM MgCl₂. Further optimization of initial crystallization conditions produced suitable cocrystals affording diffraction data from which a costructure was solved and refined to 3.2 Å resolution. Crystals were harvested by brief transfer to a drop of reservoir solution supplemented with 50% glycerol prior to plunging in liquid nitrogen.

Crystal Screening and Data Collection. Over a hundred crystals were screened using the beam light sources at SSRL and ALS. Multiple data sets were collected and indexed. The best data set was collected at the beamline measured with a PILATUS detector. Data were collected from a single crystal maintained at 100 K and 360° of data were collected using 1-degree oscillations. Data Reduction and Co-structure Determination Reflections were indexed, integrated, and scaled using HKL3000.⁶⁶ The space group was P1 with 4 molecules per asymmetric unit. The structure of ER α -LBD complexed with Compound 4 was solved by molecular replacement using the program Phenix⁶⁷ with protein coordinates from PDB 6DFN as a search model. The final model was obtained by iterative rounds of refinement (Phenix) and building (Coot⁶⁸) to a final R_{crys}/R_{free} of 0.2497/0.2893. Non-crystallographic symmetry (NCS) restraints were imposed in refinement. Coordinates and restraints for Compound 4 were generated using Phenix Elbow and added to the model after several rounds of refinement.

Cell Culture and Reagents. MCF-7 cell line was licensed from Duke University (Dr. Donald McDonnell lab) and maintained in DMEM/F12 (Gibco 11330–032), supplemented with Non-Essential Amino Acids (NEAA) (Gibco 11140–050), Na-pyruvate (Gibco 11360–070) and Fetal bovine serum (FBS) (Hyclone SH30084). CAMA-1, T47D, ZR-75–1, HCC1428 and HCC1500 were purchased from ATCC and cultured according to ATCC recommendation in RPMI-1640 complete medium. Cell culture medium and supplements, unless otherwise indicated, were purchased from either ATCC or Gibco. 4OH-tamoxifen, elacestrant, palbociclib, ribociclib, abemaciclib and alpelisib were purchased from Selleckchem. Fulvestrant and 17 β -estradiol were purchased from Sigma-Aldrich. Antibodies for ER α , PR, and anti- β -actin were from cell signaling technology (Sigma-Aldrich, V9131) as an internal control were used. Cells and tissues were lysed with RIPA buffer (Boston BioProducts) or with tissue protein extraction reagent with Halt protease inhibitors and EDTA (Thermo Fisher Scientific), respectively.

Cell Proliferation Assay. MCF-7 cells were seeded at a density of 3000 cells per well into flat clear bottom tissue cultured-treated 96-well plates (Corning) in assay medium. Assay medium components: phenol red free DMEM/F12 (Hyclone SH30272.01) 500 mL, NEAA (Gibco 11140–050) 5 mL, Na-pyruvate (Gibco 11360–070) 5 mL, restripped Charcoal stripped FBS (Gemini 100–119) 45 mL (8%) (charcoal stripped (CSS) FBS. The Charcoal stripped FBS should be restripped as follows: Add 10 mg/mL activated charcoal Norit SA 2, Dextran 70 (1 mg/mL) to FBS, Incubate at 56°C for 45 min with shaking. Centrifuge at 4°C ~ 3500 rpm for 30 min. Filter supernatant through 0.22 μm filter. Cell viability was assessed after a 6-day incubation with different compounds as indicated in the presence of 0.1 nM 17 β -estradiol (Sigma) using CellTiter-Glo (Promega) according to the manufacturer's protocol and relative luminescence units (RLU) were measured using an Envision Multilabel Reader (PerkinElmer). The RLUs of the treated samples were normalized to that of the untreated samples and cell viability was expressed as a percentage of the value of the untreated cells.

Western Blot Assay. For SERDs treatment, cells were seeded in phenol-red free media supplemented with charcoal-stripped FBS. Forty-eight h later, cells were treated with SERDs at the indicated

concentrations. For other drug treatments, cells were seeded in regular culture medium. Cells were lysed in RIPA buffer protease and phosphoprotease inhibitors (Thermo Fisher Scientific) after 24 or 48 h of treatment, and total proteins were separated by SDS-PAGE and immunoblotted using antibodies as indicated. For pharmacodynamic studies using tumor samples from xenograft studies, flash-frozen tumors were pulverized and tissue was lysed in RIPA buffer. Total protein was analyzed by Western blot.

Mouse and Rat Pharmacokinetic Studies (PH-DMPK-KAP-16–035 and PH-DMPK-KAP-16–036, Respectively). Female CD1 mice (20–30 g) or female Sprague–Dawley rats (200–300 g) were randomly grouped. A group of 3 animals was administered the test compound at an indicated dose. The IV arm was dosed at 3 mg/kg using a formulation of DMSO/PEG400/150 mM glycine (pH 9) (5/10/85). The oral arm was dosed at 10 mg/kg using a formulation of PEG400/PVP/Tween 80/0.5% CMC in water (9/0.5/0.5/90). The blood samples were collected at 0.25, 0.5, 1, 2, 4, 8, 12, and 24 h time points. The concentrations of test compounds in plasma samples were determined by using LC–MS/MS. Standard curves were plotted based on concentrations of the samples in a suitable range. Pharmacokinetic parameters were calculated according to a drug concentration–time curve using a noncompartmental method by WinNonLin (Phoenix, version 6.1) or similar software.

Dog Pharmacokinetic Study (Pharmaron Study: 66704–16–033). Female beagle dogs were randomly grouped. A group of three animals was administered the test compound at an indicated dose. The IV arm was dosed at 3 mg/kg using a formulation of EtOH/PEG400/30%HP β -CD (10/40/50). The oral arm was dosed at 10 mg/kg using a formulation of PEG400/PVP/Tween 80/0.5% CMC in water (9/0.5/0.5/90). The blood samples for the IV arm were collected at predose, 5, 15, 30 min, 1, 2, 4, 8, 12, and 24 h time points. The blood samples for the PO arm were collected at predose, 15, 30 min, 1, 2, 4, 6, 8, 12, and 24 h time points. The concentrations of the test compound in plasma samples were determined by using LC–MS/MS. Standard curves were plotted based on concentrations of the samples in a suitable range. Pharmacokinetic parameters were calculated according to a drug concentration–time curve using a noncompartmental method by WinNonLin (Phoenix, version 6.1) or similar software.

In Vivo Efficacy Studies. Animal studies were performed according to guidelines approved by the Institutional Animal Care and Use Committee (IACUC) of CrownBio or Horizon following the guidance of the Association for Assessment and Accreditation of Laboratory Animal Care (AAALAC). For MCF-7 model (CrownBio study#: E1664-U1701), mice were inoculated subcutaneously on the second right mammary fat pad with the single cell suspension of 95% viable tumor cells (1.5×10^7) in 200 μL medium Matrigel mixture (1:1 ratio) without serum for the tumor development. The treatments were started when mean tumor size reached ~ 200 mm³. Mice were randomized into 10 groups. In addition, estradiol benzoate injection was delivered by s.c. (40 μg /20 μL , twice weekly). For WHIM20 PDX study (Horizon Study #0454), female athymic nude mice were implanted with a single cell suspension of 1.5×10^6 WHIM20 cells, passage 10. The cells were mixed 1:1 with PBS:Matrigel (Corning ref 354234, lot#0090009) in a total volume of 100 μL /mouse. Once tumors reached approximately 100–300 mm³, mice were randomized by tumor volume into 1 of 10 treatment groups (8 mice/group) using Bioptron's Tumor Manager software.

Human Clinical Trials. The ZN-c5–001 clinical trial (NCT03560531) was conducted in accordance with United States ethical guidelines (i.e., U.S. Common Rule) and the Declaration of Helsinki, Good Clinical Practice, and all federal, state regulatory guidelines and approved by Western Institutional Review Board and NYSDOH Institutional Review Board (IRB). In the ZN-c5–001 study, ZN-c5 was administered once daily or twice daily with dose ranging from 25 mg to 300 mg per day in 28-day cycles to patients enrolled under the protocol. Plasma samples were collected at cycle 1, day 1 (single dose) or cycle 1, day 15 (steady state) for PK analysis (MicroConstant). All patients provided written informed consent prior to study enrollment.

■ ASSOCIATED CONTENT

■ Supporting Information

The Supporting Information is available free of charge at <https://pubs.acs.org/doi/10.1021/acs.jmedchem.5c00887>.

Characterization: HPLC traces of compounds 1–6 and ¹H-NMR spectra of compounds 1–6 (PDF)

SMILES molecular formula strings with compound data information (CSV)

■ Accession Codes

Atomic coordinates and structure factors for the ER α LBD complexed with compound 4 (PDB code: 9ECK) have been deposited in the Protein Data Bank with accession code 9ECK. Authors will release the atomic coordinates upon article publication.

■ AUTHOR INFORMATION

■ Corresponding Author

Sayee G. Hegde – Zentalis Pharmaceuticals, San Diego, California 92121, United States; orcid.org/0009-0001-4232-1019; Email: sghegde108@gmail.com

■ Authors

Peter Q. Huang – Zentalis Pharmaceuticals, San Diego, California 92121, United States

Kevin D. Bunker – Zentalis Pharmaceuticals, San Diego, California 92121, United States; orcid.org/0009-0004-0537-9336

Chad D. Hopkins – Zentalis Pharmaceuticals, San Diego, California 92121, United States

Deborah H. Slee – Zentalis Pharmaceuticals, San Diego, California 92121, United States

Mehmet Kahraman – Zentalis Pharmaceuticals, San Diego, California 92121, United States

Joseph Pinchman – Zentalis Pharmaceuticals, San Diego, California 92121, United States

Rakesh K. Sit – Zentalis Pharmaceuticals, San Diego, California 92121, United States

Christian C. Lee – Zentalis Pharmaceuticals, San Diego, California 92121, United States

Michael Rutgard – Zentalis Pharmaceuticals, San Diego, California 92121, United States

Ahmed A. Samatar – Zentalis Pharmaceuticals, San Diego, California 92121, United States

Jiali Li – Zentalis Pharmaceuticals, San Diego, California 92121, United States

Jianhui Ma – Zentalis Pharmaceuticals, San Diego, California 92121, United States; orcid.org/0000-0002-9374-2673

Hooman Izadi – Zentalis Pharmaceuticals, San Diego, California 92121, United States

Frank Q. Han – Structure Based Design, Inc., San Diego, California 92121, United States

Alex Chao – Structure Based Design, Inc., San Diego, California 92121, United States; orcid.org/0000-0003-2134-1632

Complete contact information is available at:

<https://pubs.acs.org/doi/10.1021/acs.jmedchem.5c00887>

■ Notes

The authors declare no competing financial interest.

■ ACKNOWLEDGMENTS

The authors are grateful to Dr. Guobao Zhang and Dr. Martin Rowbottom for excellent discussions and valuable contributions

regarding the manuscript. The authors would also like to thank the Advanced Light Source at Berkeley National Laboratories (ALS) and the Stanford Synchrotron Radiation Lightsource (SSRL) and their staff for their help with data collection.

■ ABBREVIATIONS USED

ADME:absorption, distribution, metabolism, and excretion; AUC:area under the curve; CDX:cell-line-derived xenograft; Cl_{int}:intrinsic clearance; CYP:cytochrome P450; HP- β -CD:(2-hydroxypropyl)- β -cyclodextrin; IC₅₀:50% inhibitory concentration; log D:octanol/buffer (pH 7.4) distribution coefficient; PDB:protein data bank; PK:pharmacokinetic; PDX:patient-derived xenograft; PPB:plasma protein binding; SAR:structure–activity relationship; SFC:supercritical fluid chromatography

■ REFERENCES

- (1) Bray, F.; Ferlay, J.; Soerjomataram, I.; Siegel, R. L.; Torre, L. A.; Jemal, A. Global Cancer Statistics 2018: GLOBOCAN Estimates of Incidence and Mortality Worldwide for 36 Cancers in 185 Countries. *Ca Cancer J. Clin* **2018**, *68* (6), 394–424.
- (2) Haines, C. N.; Wardell, S. E.; McDonnell, D. P. Current and Emerging Estrogen Receptor-Targeted Therapies for the Treatment of Breast Cancer. *Essays Biochem* **2021**, *65* (6), 985–1001.
- (3) McDonnell, D. P.; Wardell, S. E.; Norris, J. D. Oral Selective Estrogen Receptor Downregulators (SERDs), a Breakthrough Endocrine Therapy for Breast Cancer. *J. Med. Chem.* **2015**, *58* (12), 4883–4887.
- (4) Patel, R.; Klein, P.; Tiersten, A.; Sparano, J. A. An Emerging Generation of Endocrine Therapies in Breast Cancer: A Clinical Perspective. *npj Breast Cancer* **2023**, *9* (1), 20.
- (5) Mottamal, M.; Kang, B.; Peng, X.; Wang, G. From Pure Antagonists to Pure Degraders of the Estrogen Receptor: Evolving Strategies for the Same Target. *ACS Omega* **2021**, *6* (14), 9334–9343.
- (6) Neupane, N.; Bawek, S.; Gurusinge, S.; Ghaffary, E. M.; Mirmosayyeb, O.; Thapa, S.; Falkson, C.; O'Regan, R.; Dhakal, A. Oral SERD, a Novel Endocrine Therapy for Estrogen Receptor-Positive Breast Cancer. *Cancers* **2024**, *16* (3), 619.
- (7) Howell, A.; Robertson, J. F. R.; Albano, J. Q.; Aschermannova, A.; Mauriac, L.; Kleeberg, U. R.; Vergote, I.; Erikstein, B.; Webster, A.; Morris, C. Fulvestrant, Formerly ICI 182,780, Is as Effective as Anastrozole in Postmenopausal Women With Advanced Breast Cancer Progressing After Prior Endocrine Treatment. *J. Clin. Oncol.* **2002**, *20* (16), 3396–3403.
- (8) Robertson, J. F.; Nicholson, R. L.; Bundred, N. J.; Anderson, E.; Rayter, Z.; Dowsett, M.; Fox, J. N.; Gee, J. M. W.; Webster, A.; Wakeling, A. E.; Morris, C.; Dixon, M. Comparison of the Short-Term Biological Effects of 7 α -[9-(4,4,5,5,5-pentafluoropentylsulfinyl)-nonyl]estra-1,3,5, (10)-triene-3,17 β -diol (Faslodex) versus tamoxifen in postmenopausal women with primary breast cancer. *Cancer Res.* **2001**, *61* (18), 6739–6746.
- (9) Robertson, J. F. R.; Harrison, M. Fulvestrant: Pharmacokinetics and Pharmacology. *Br. J. Cancer* **2004**, *90* (Suppl 1), S7–S10.
- (10) McDonnell, D. P.; Wardell, S. E. The molecular mechanisms underlying the pharmacological actions of ER modulators: implications for new drug discovery in breast cancer. *Curr. Opin. Pharmacol.* **2010**, *10*, 620–628.
- (11) Wardell, S. E.; Marks, J. R.; McDonnell, D. P. The Turnover of Estrogen Receptor α by the Selective Estrogen Receptor Degradator (SERD) Fulvestrant Is a Saturable Process That Is Not Required for Antagonist Efficacy. *Biochem. Pharmacol.* **2011**, *82* (2), 122–130.
- (12) Berry, N. B.; Fan, M.; Nephew, K. P. Estrogen Receptor- α Hinge-Region Lysines 302 and 303 Regulate Receptor Degradation by the Proteasome. *Mol. Endocrinol.* **2008**, *22* (7), 1535–1551.
- (13) Tecalco-Cruz, A. C.; Ramírez-Jarquín, J. O. Polyubiquitination Inhibition of Estrogen Receptor Alpha and Its Implications in Breast Cancer. *World J. Clin. Oncol.* **2018**, *9* (4), 60–70.

- (14) Nardone, A.; Angelis, C. D.; Trivedi, M. V.; Osborne, C. K.; Schiff, R. The Changing Role of ER in Endocrine Resistance. *Breast* **2015**, *24*, S60–S66.
- (15) Wijayaratne, A. L.; McDonnell, D. P. The Human Estrogen Receptor- α Is a Ubiquitinated Protein Whose Stability Is Affected Differentially by Agonists, Antagonists, and Selective Estrogen Receptor Modulators. *J. Biol. Chem.* **2001**, *276* (38), 35684–35692.
- (16) Tateishi, Y.; Kawabe, Y.; Chiba, T.; Murata, S.; Ichikawa, K.; Murayama, A.; Tanaka, K.; Baba, T.; Kato, S.; Yanagisawa, J. Ligand-dependent Switching of Ubiquitin–Proteasome Pathways for Estrogen Receptor. *EMBO J.* **2004**, *23* (24), 4813–4823.
- (17) Wittmann, B. M.; Sherk, A.; McDonnell, D. P. Definition of Functionally Important Mechanistic Differences among Selective Estrogen Receptor Down-Regulators. *Cancer Res.* **2007**, *67* (19), 9549–9560.
- (18) Knox, A. K.; Kalchschmid, C.; Schuster, D.; Gaggia, F.; Gust, R. Heterodimeric GW7604 Derivatives: Modification of the Pharmacological Profile by Additional Interactions at the Coactivator Binding Site. *J. Med. Chem.* **2021**, *64* (9), 5766–5786.
- (19) Lai, A.; Kahraman, M.; Govek, S.; Nagasawa, J.; Bonnefous, C.; Julien, J.; Douglas, K.; Sensintaffar, J.; Lu, N.; Lee, K.; Aparicio, A.; Kaufman, J.; Qian, J.; Shao, G.; Prudente, R.; Moon, M. J.; Joseph, J. D.; Darimont, B.; Brigham, D.; Grillot, K.; Heyman, R.; Rix, P. J.; Hager, J. H.; Smith, N. D. Identification of GDC-0810 (ARN-810), an Orally Bioavailable Selective Estrogen Receptor Degradator (SERD) That Demonstrates Robust Activity in Tamoxifen-Resistant Breast Cancer Xenografts. *J. Med. Chem.* **2015**, *58* (12), 4888–4904.
- (20) Savi, C. D.; Bradbury, R. H.; Rabow, A. A.; Norman, R. A.; Almeida, C. de; Andrews, D. M.; Ballard, P.; Buttar, D.; Callis, R. J.; Currie, G. S.; Curwen, J. O.; Davies, C. D.; Donald, C. S.; Feron, L. J. L.; Gingell, H.; Glossop, S. C.; Hayter, B. R.; Hussain, S.; Karoutchi, G.; Lamont, S. G.; MacFaul, P.; Moss, T. A.; Pearson, S. E.; Tonge, M.; Walker, G. E.; Weir, H. M.; Wilson, Z. Optimization of a Novel Binding Motif to (E)-3-(3,5-Difluoro-4-((1R,3R)-2-(2-Fluoro-2-Methylpropyl)-3-Methyl-2,3,4,9-tetrahydro-1H-pyrido[3,4-b]Indol-1-Yl)Phenyl)-Acrylic Acid (AZD9496), a Potent and Orally Bioavailable Selective Estrogen Receptor Downregulator and Antagonist. *J. Med. Chem.* **2015**, *58* (20), 8128–8140.
- (21) Tria, G. S.; Abrams, T.; Baird, J.; Burks, H. E.; Firestone, B.; Gaither, L. A.; Hamann, L. G.; He, G.; Kirby, C. A.; Kim, S.; Lombardo, F.; Macchi, K. J.; McDonnell, D. P.; Mishina, Y.; Norris, J. D.; Nunez, J.; Springer, C.; Sun, Y.; Thomsen, N. M.; Wang, C.; Wang, J.; Yu, B.; Tiong-Yip, C.-L.; Peukert, S. Discovery of LSZ102, a Potent, Orally Bioavailable Selective Estrogen Receptor Degradator (SERD) for the Treatment of Estrogen Receptor Positive Breast Cancer. *J. Med. Chem.* **2018**, *61* (7), 2837–2864.
- (22) El-Ahmad, Y.; Tabart, M.; Halley, F.; Certal, V.; Thompson, F.; Filoche-Rommé, B.; Gruss-Leleu, F.; Muller, C.; Brollo, M.; Fabien, L.; Loyau, V.; Bertin, L.; Richepin, P.; Pilorge, F.; Desmazeau, P.; Girardet, C.; Beccari, C.; Louboutin, A.; Lebourg, G.; Le-Roux, J.; Terrier, C.; Vallée, F.; Steier, V.; Mathieu, M.; Rak, A.; Abecassis, P.-Y.; Vicat, P.; Benard, T.; Bouaboula, M.; Sun, F.; Shomali, M.; Hebert, A.; Levit, M.; Cheng, H.; Courjaud, A.; Ginesty, C.; Perrault, C.; Garcia-Echeverria, C.; McCort, G.; Schio, L. Discovery of 6-(2,4-Dichlorophenyl)-5-[4-[(3S)-1-(3-Fluoropropyl)Pyrrolidin-3-Yl]Oxyphenyl]-8,9-dihydro-7H-benzo[7]Annulene-2-Carboxylic Acid (SAR439859), a Potent and Selective Estrogen Receptor Degradator (SERD) for the Treatment of Estrogen-Receptor-Positive Breast Cancer. *J. Med. Chem.* **2020**, *63* (2), 512–528.
- (23) Liang, J.; Zbieg, J. R.; Blake, R. A.; Chang, J. H.; Daly, S.; DiPasquale, A. G.; Friedman, L. S.; Gelzleichter, T.; Gill, M.; Giltman, J. M.; Goodacre, S.; Guan, J.; Hartman, S. J.; Ingalla, E. R.; Kategaya, L.; Kiefer, J. R.; Kleinheinz, T.; Labadie, S. S.; Lai, T.; Li, J.; Liao, J.; Liu, Z.; Mody, V.; McLean, N.; Metcalfe, C.; Nannini, M. A.; Oeh, J.; O'Rourke, M. G.; Ortwine, D. F.; Ran, Y.; Ray, N. C.; Roussel, F.; Sambrone, A.; Sampath, D.; Schutt, L. K.; Vinogradova, M.; Wai, J.; Wang, T.; Wertz, I. E.; White, J. R.; Yeap, S. K.; Young, A.; Zhang, B.; Zheng, X.; Zhou, W.; Zhong, Y.; Wang, X. GDC-9545 (Giredestrant): A Potent and Orally Bioavailable Selective Estrogen Receptor Antagonist and Degradator with an Exceptional Preclinical Profile for ER+ Breast Cancer. *J. Med. Chem.* **2021**, *64* (16), 11841–11856.
- (24) Scott, J. S.; Moss, T. A.; Balazs, A.; Barlaam, B.; Breed, J.; Carbajo, R. J.; Chiarparin, E.; Davey, P. R. J.; Delpuech, O.; Fawell, S.; Fisher, D. I.; Gagra, S.; Gangl, E. T.; Grebe, T.; Greenwood, R. D.; Hande, S.; Hatoum-Mokdad, H.; Herlihy, K.; Hughes, S.; Hunt, T. A.; Huynh, H.; Janbon, S. L. M.; Johnson, T.; Kavanagh, S.; Klinowska, T.; Lawson, M.; Lister, A. S.; Marden, S.; McGinnity, D. F.; Morrow, C. J.; Nissink, J. W. M.; O'Donovan, D. H.; Peng, B.; Polanski, R.; Stead, D. S.; Stokes, S.; Thakur, K.; Throner, S. R.; Tucker, M. J.; Varnes, J.; Wang, H.; Wilson, D. M.; Wu, D.; Wu, Y.; Yang, B.; Yang, W. Discovery of AZD9833, a Potent and Orally Bioavailable Selective Estrogen Receptor Degradator and Antagonist. *J. Med. Chem.* **2020**, *63* (23), 14530–14559.
- (25) Scott, J. S.; Stead, D.; Barlaam, B.; Breed, J.; Carbajo, R. J.; Chiarparin, E.; Cureton, N.; Davey, P. R. J.; Fisher, D. I.; Gangl, E. T.; Grebe, T.; Greenwood, R. D.; Hande, S.; Hatoum-Mokdad, H.; Hughes, S. J.; Hunt, T. A.; Johnson, T.; Kavanagh, S. L.; Klinowska, T. C. M.; Lerner, C. J. B.; Lawson, M.; Lister, A. S.; Longmire, D.; Marden, S.; McGuire, T. M.; McMillan, C.; McMurray, L.; Morrow, C. J.; Nissink, J. W. M.; Moss, T. A.; O'Donovan, D. H.; Polanski, R.; Stokes, S.; Thakur, K.; Trueman, D.; Truman, C.; Tucker, M. J.; Wang, H.; Whalley, N.; Wu, D.; Wu, Y.; Yang, B.; Yang, W. Discovery of a Potent and Orally Bioavailable Zwitterionic Series of Selective Estrogen Receptor Degradator-Antagonists. *J. Med. Chem.* **2023**, *66* (4), 2918–2945.
- (26) Bhagwat, S. V.; Mur, C.; Vandekopple, M.; Zhao, B.; Shen, W.; Marugán, C.; Capen, A.; Kindler, L.; Stephens, J. R.; Huber, L.; Castanares, M. A.; Garcia-Tapia, D.; Cohen, J. D.; Bastian, J.; Mattioni, B.; Yuen, E.; Baker, T. K.; Cruz, V. R.; Fei, D.; Manro, J. R.; Pulliam, N.; Dowless, M. S.; Ruiz, M. J. O.; Yu, C.; Puca, L.; Klippel, A.; Bacchion, F.; Ismail-Khan, R.; Rodrik-Outmezguine, V.; Peng, S.-B.; Lallena, M. J.; Gong, X.; Dios, A. de Imlunestrant Is an Oral, Brain-Penetrant Selective Estrogen Receptor Degradator with Potent Antitumor Activity in ESR1 Wildtype and Mutant Breast Cancer. *Cancer Res.* **2025**, *85* (4), 777–790.
- (27) Parisian, A. D.; Barratt, S. A.; Hodges-Gallagher, L.; Ortega, F. E.; Peña, G.; Sapugay, J.; Robello, B.; Sun, R.; Kulp, D.; Palanisamy, G. S.; Myles, D. C.; Kushner, P. J.; Harmon, C. L. Palazestrant (OP-1250), a Complete Estrogen Receptor Antagonist, Inhibits Wild-Type and Mutant ER-Positive Breast Cancer Models as Monotherapy and in Combination. *Mol. Cancer Ther.* **2024**, *23* (3), 285–300.
- (28) Garner, F.; Shomali, M.; Paquin, D.; Lyttle, C. R.; Hattersley, G. RAD1901. *Anti-Cancer Drugs* **2015**, *26* (9), 948–956.
- (29) Scott, J. S.; Klinowska, T. C. M. Selective Estrogen Receptor Degradators (SERDs) and Covalent Antagonists (SERCAs): A Patent Review (July 2021–December 2023). *Expert Opin. Ther. Pat.* **2024**, *34* (5), 333–350.
- (30) Fierce Biotech. <https://www.fiercebiotech.com/biotech/roche-dumps-lead-asset-from-its-725m-seragon-buy> (accessed Apr 27, 2017).
- (31) Astra Zeneca corporate site. <https://www.astrazenecaclinicaltrials.com/study/D6090C00005/>.
- (32) Bapiro, T. E.; Sykes, A.; Martin, S.; Davies, M.; Yates, J. W.; Hoch, M.; Rollison, H. E.; Jones, B. Complete Substrate Inhibition of Cytochrome P450 2C8 by AZD9496, an Oral Selective Estrogen Receptor Degradator. *Drug Metab. Dispos.* **2018**, *46* (9), 1268–1276.
- (33) Hamilton, E. P.; Patel, M. R.; Armstrong, A. C.; Baird, R. D.; Jhaveri, K.; Hoch, M.; Klinowska, T.; Lindemann, J. P. O.; Morgan, S. R.; Schiavon, G.; Weir, H. M.; Im, S.-A. A First-in-Human Study of the New Oral Selective Estrogen Receptor Degradator AZD9496 for ER+/HER2–Advanced Breast Cancer. *Clin. Cancer Res.* **2018**, *24* (15), 3510–3518.
- (34) Wu, C.; Decker, E. R.; Blok, N.; Bui, H.; You, T. J.; Wang, J.; Bourgoynne, A. R.; Knowles, V.; Berens, K. L.; Holland, G. W.; Brock, T. A.; Dixon, R. A. F. Discovery, Modeling, and Human Pharmacokinetics of N-(2-Acetyl-4,6-Dimethylphenyl)-3-(3,4-Dimethylisoxazol-5-Ylsulfamoyl)Thiophene-2-Carboxamide (TBC3711), a Second Generation, ETA Selective, and Orally Bioavailable Endothelin Antagonist. *J. Med. Chem.* **2004**, *47* (8), 1969–1986.

- (35) Stepan, A. F.; Mascitti, V.; Beaumont, K.; Kalgutkar, A. S. Metabolism-Guided Drug Design. *MedChemComm* **2013**, *4* (4), 631–652.
- (36) Wiberg, K. B.; Connor, D. S. Bicyclo[1.1.1]Pentane 1. *J. Am. Chem. Soc.* **1966**, *88* (19), 4437–4441.
- (37) Bunker, K. D.; Sach, N. W.; Huang, Q.; Richardson, P. F. Scalable Synthesis of 1-Bicyclo[1.1.1]Pentylamine via a Hydrohydrazination Reaction. *Org. Lett.* **2011**, *13* (17), 4746–4748.
- (38) Lopchuk, J. M.; Fjelbye, K.; Kawamata, Y.; Malins, L. R.; Pan, C.-M.; Gianatassio, R.; Wang, J.; Prieto, L.; Bradow, J.; Brandt, T. A.; Collins, M. R.; Elleraas, J.; Ewanicki, J.; Farrell, W.; Fadeyi, O. O.; Gallego, G. M.; Mousseau, J. J.; Oliver, R.; Sach, N. W.; Smith, J. K.; Spangler, J. E.; Zhu, H.; Zhu, J.; Baran, P. S. Strain-Release Heteroatom Functionalization: Development, Scope, and Stereospecificity. *J. Am. Chem. Soc.* **2017**, *139* (8), 3209–3226.
- (39) Gianatassio, R.; Lopchuk, J. M.; Wang, J.; Pan, C.-M.; Malins, L. R.; Prieto, L.; Brandt, T. A.; Collins, M. R.; Gallego, G. M.; Sach, N. W.; Spangler, J. E.; Zhu, H.; Zhu, J.; Baran, P. S. Strain-Release Amination. *Science* **2016**, *351* (6270), 241–246.
- (40) Shire, B. R.; Anderson, E. A. Conquering the Synthesis and Functionalization of Bicyclo[1.1.1]pentanes. *J. Am. Chem. Soc. Au* **2023**, *3*, 1539–1553.
- (41) Stepan, A. F.; Subramanyam, C.; Efremov, I. V.; Dutra, J. K.; O'Sullivan, T. J.; DiRico, K. J.; McDonald, W. S.; Won, A.; Dorff, P. H.; Nolan, C. E.; Becker, S. L.; Pustilnik, L. R.; Riddell, D. R.; Kauffman, G. W.; Kormos, B. L.; Zhang, L.; Lu, Y.; Capetta, S. H.; Green, M. E.; Karki, K.; Sibley, E.; Atchison, K. P.; Hallgren, A. J.; Oborski, C. E.; Robshaw, A. E.; Sneed, B.; O'Donnell, C. J. Application of the Bicyclo[1.1.1]Pentane Motif as a Nonclassical Phenyl Ring Bioisostere in the Design of a Potent and Orally Active γ -Secretase Inhibitor. *J. Med. Chem.* **2012**, *55* (7), 3414–3424.
- (42) Makarov, I. S.; Brocklehurst, C. E.; Karaghiosoff, K.; Koch, G.; Knochel, P. Synthesis of Bicyclo[1.1.1]Pentane Bioisosteres of Internal Alkynes and para-Disubstituted Benzenes from [1.1.1]Propellane. *Angewandte Chemie Int. Ed.* **2017**, *56* (41), 12774–12777.
- (43) Westphal, M. V.; Wolfstädter, B. T.; Plancher, J.; Gatfield, J.; Carreira, E. M. Evaluation of tert-Butyl Isosteres: Case Studies of Physicochemical and Pharmacokinetic Properties, Efficacies, and Activities. *ChemMedChem* **2015**, *10* (3), 461–469.
- (44) Pellicciari, R.; Raimondo, M.; Marinozzi, M.; Natalini, B.; Costantino, G.; Thomsen, C. (S)-(+)-2-(3'-Carboxybicyclo[1.1.1]-Pentyl)-Glycine, a Structurally New Group I Metabotropic Glutamate Receptor Antagonist. *J. Med. Chem.* **1996**, *39* (15), 2874–2876.
- (45) Lovering, F.; Bikker, J.; Humblet, C. Escape from Flatland: Increasing Saturation as an Approach to Improving Clinical Success. *J. Med. Chem.* **2009**, *52* (21), 6752–6756.
- (46) Pu, Q.; Zhang, H.; Guo, L.; Cheng, M.; Doty, A. C.; Ferguson, H.; Fradera, X.; Lesburg, C. A.; McGowan, M. A.; Miller, J. R.; Geda, P.; Song, X.; Otte, K.; Sciammetta, N.; Solban, N.; Yu, W.; Sloman, D. L.; Zhou, H.; Lammens, A.; Neumann, L.; Bennett, D. J.; Pasternak, A.; Han, Y. Discovery of Potent and Orally Available Bicyclo[1.1.1]-Pentane-Derived Indoleamine-2,3-Dioxygenase 1 (IDO1) Inhibitors. *ACS Med. Chem. Lett.* **2020**, *11* (8), 1548–1554.
- (47) Goh, Y. L.; Cui, Y. T.; Pendharkar, V.; Adsool, V. A. Toward Resolving the Resveratrol Conundrum: Synthesis and In Vivo Pharmacokinetic Evaluation of BCP-Resveratrol. *ACS Med. Chem. Lett.* **2017**, *8* (5), 516–520.
- (48) Meason, N. D.; Down, K. D.; Hirst, D. J.; Jamieson, C.; Manas, E. S.; Patel, V. K.; Somer, D. O. Investigation of a Bicyclo[1.1.1]pentane as a Phenyl Replacement within an LpPLA2 Inhibitor. *ACS Med. Chem. Lett.* **2016**, *8* (1), 43–48.
- (49) Weir, H. M.; Bradbury, R. H.; Lawson, M.; Rabow, A. A.; Buttar, D.; Callis, R. J.; Curwen, J. O.; Almeida, C. de; Ballard, P.; Hulse, M.; Donald, C. S.; Feron, L. J. L.; Karoutchi, G.; MacFaul, P.; Moss, T.; Norman, R. A.; Pearson, S. E.; Tonge, M.; Davies, G.; Walker, G. E.; Wilson, Z.; Rowlinson, R.; Powell, S.; Sadler, C.; Richmond, G.; Ladd, B.; Pazolli, E.; Mazzola, A. M.; D'Cruz, C.; Savi, C. D. AZD9496: An Oral Estrogen Receptor Inhibitor That Blocks the Growth of ER-Positive and ESR1-Mutant Breast Tumors in Preclinical Models. *Cancer Res.* **2016**, *76* (11), 3307–3318.
- (50) Sweeney, E. E.; McDaniel, R. E.; Maximov, P. Y.; Fan, P.; Jordan, V. C. Models and Mechanisms of Acquired Antihormone Resistance in Breast Cancer: Significant Clinical Progress despite Limitations. *hmbci* **2012**, *9* (2), 143–163.
- (51) Samatar, A. A.; Li, J.; Hegde, S.; Huang, P.; Ma, J.; Bunker, K.; Winkler, R.; Donate, F.; Sergeeva, M. Discovery of ZN-cS, a novel potent and oral selective estrogen receptor degrader. *Cancer Res.* **2020**, *80* (Suppl. S16), 4373.
- (52) Nardone, A.; Weir, H.; Delpuech, O.; Brown, H.; Angelis, C. D.; Cataldo, M. L.; Fu, X.; Shea, M. J.; Mitchell, T.; Veeraraghavan, J.; Nagi, C.; Pilling, M.; Rimawi, M. F.; Trivedi, M.; Hilsenbeck, S. G.; Chamness, G. C.; Jeselsohn, R.; Osborne, C. K.; Schiff, R. The Oral Selective Oestrogen Receptor Degradator (SERD) AZD9496 Is Comparable to Fulvestrant in Antagonising ER and Circumventing Endocrine Resistance. *Br. J. Cancer* **2019**, *120* (3), 331–339.
- (53) Joseph, J. D.; Darimont, B.; Zhou, W.; Arrazate, A.; Young, A.; Ingalla, E.; Walter, K.; Blake, R. A.; Nonomiya, J.; Guan, Z.; Kategaya, L.; Govek, S. P.; Lai, A. G.; Kahraman, M.; Brigham, D.; Sensintaffar, J.; Lu, N.; Shao, G.; Qian, J.; Grillot, K.; Moon, M.; Prudente, R.; Bischoff, E.; Lee, K.-J.; Bonnefous, C.; Douglas, K. L.; Julien, J. D.; Nagasawa, J. Y.; Aparicio, A.; Kaufman, J.; Haley, B.; Giltane, J. M.; Wertz, I. E.; Lackner, M. R.; Nannini, M. A.; Sampath, D.; Schwarz, L.; Manning, H. C.; Tantawy, M. N.; Arteaga, C. L.; Heyman, R. A.; Rix, P. J.; Friedman, L.; Smith, N. D.; Metcalfe, C.; Hager, J. H. The Selective Estrogen Receptor Downregulator GDC-0810 Is Efficacious in Diverse Models of ER+ Breast Cancer. *Elife* **2016**, *5*, No. e15828.
- (54) Guan, J.; Zhou, W.; Hafner, M.; Blake, R. A.; Chalouni, C.; Chen, I. P.; Bruyn, T. D.; Giltane, J. M.; Hartman, S. J.; Heidersbach, A.; Houtman, R.; Ingalla, E.; Kategaya, L.; Kleinheinz, T.; Li, J.; Martin, S. E.; Modrusan, Z.; Nannini, M.; Oeh, J.; Ubhayakar, S.; Wang, X.; Wertz, I. E.; Young, A.; Yu, M.; Sampath, D.; Hager, J. H.; Friedman, L. S.; Daemen, A.; Metcalfe, C. Therapeutic Ligands Antagonize Estrogen Receptor Function by Impairing Its Mobility. *Cell* **2019**, *178* (4), 949–963.e18.
- (55) Lawson, M.; Cureton, N.; Ros, S.; Cheraghchi-Bashi-Astaneh, A.; Urošević, J.; D'Arcy, S.; Delpuech, O.; DuPont, M.; Fisher, D. I.; Gangl, E. T.; Lewis, H.; Trueman, D.; Wali, N.; Williamson, S. C.; Moss, J.; Montaudon, E.; Derrien, H.; Marangoni, E.; Miragaia, R. J.; Gargica, S.; Gutierrez, P. M.; Moss, T.; Maglennon, G. A.; Sutton, D.; Polanski, R.; Rosen, A.; Cairns, J.; Zhang, P.; Sánchez-Guixé, M.; Serra, V.; Critchlow, S. E.; Scott, J. S.; Lindemann, J. P. O.; Barry, S. T.; Klinowska, T.; Morrow, C. J.; Carnevali, L. S. The Next-Generation Oral Selective Estrogen Receptor Degradator Camizestrant (AZD9833) Suppresses ER+ Breast Cancer Growth and Overcomes Endocrine and CDK4/6 Inhibitor Resistance. *Cancer Res.* **2023**, *83* (23), 3989–4004.
- (56) Ma, J.; Li, J.; Hegde, S.; Sergeeva, M.; Thuong, T.; Chakraborty, B.; Wardell, S.; McDonnell, D.; Donate, F.; Huang, P.; Bunker, K.; Lacker, M. R.; Samatar, A. A. The Selective Estrogen Receptor ZN-cS has Broad Anti-Tumor Activity in Wild-Type and Mutant ER-Positive Breast Cancer Models. *Submitted to Molecular Cell Therapeutics*, **2025** (unpublished results).
- (57) Time-dependent inhibition of 2C8 was not observed with compound 4. Compound 4 is primarily metabolized by 3A4 unlike AZD9496 (primarily metabolized by 2C8), and therefore was not expected to exhibit non-linear human PK due to 2C8 inhibition.
- (58) Tanenbaum, D. M.; Wang, Y.; Williams, S. P.; Sigler, P. B. Crystallographic Comparison of the Estrogen and Progesterone Receptor's Ligand Binding Domains. *Proc. Natl. Acad. Sci. U. S. A.* **1998**, *95* (11), 5998–6003.
- (59) Degorce, S. L.; Bailey, A.; Callis, R.; Savi, C. D.; Ducray, R.; Lamont, G.; MacFaul, P.; Maudet, M.; Martin, S.; Morgentin, R.; Norman, R. A.; Peru, A.; Pink, J. H.; Plé, P. A.; Roberts, B.; Scott, J. S. Investigation of (E)-3-[4-(2-Oxo-3-Aryl-Chromen-4-Yl)Oxyphenyl]-Acrylic Acids as Oral Selective Estrogen Receptor Down-Regulators. *J. Med. Chem.* **2015**, *58* (8), 3522–3533.
- (60) The PyMOL Molecular Graphics System, Version 3.0; Schrödinger, LLC, 2025.

- 1412 (61) *Molecular Operating Environment (MOE)*; 2022.02 Chemical
1413 Computing Group ULC: Montreal, Canada, 2024.
- 1414 (62) Zentalis ZN-c5 SERD patent applications: (a) Huang, P. Q.;
1415 Slee, D. H.; Hegde, S. G.; Hopkins, C. D.; Bunker, K. D.; Pinchman, J.
1416 R.; Sit, R. K. Preparation of tetrahydropyridindolylcycloalkylacrylic
1417 acid derivatives and analogs for use as estrogen receptor modulators.
1418 WO2017172957 A1, 2017. (b) Huang, P. Q.; Hegde, S. G.; Bunker, K.
1419 D.; Knight, J.; Slee, D. H. The salts and forms of an estrogen receptor
1420 modulator. WO2021091819 A1, 2021. (c) Huang, P. Q.; Hegde, S. G.;
1421 Bunker, K. D.; Knight, J.; Pinchman, J. R.; Unni, A. K.; Sit, R. S.; Zhu, S.;
1422 Hopkins, C. D.; Scott, I. Preparation of an selective estrogen receptor
1423 degrader. WO2021216671 A1, 2021.
- 1424 (63) Foldi, J.; Beumer, J. H. Pharmacology and Pharmacokinetics of
1425 Elacestrant. *Cancer Chemother Pharmacol.* **2023**, 92 (2), 157–163.
- 1426 (64) Jhaveri, K.; Juric, D.; Yap, Y. S.; Cresta, S.; Layman, R. M.;
1427 Duhoux, F. P.; Terret, C.; Takahashi, S.; Huober, J.; Kundamal, N.;
1428 Sheng, Q.; Balbin, A.; Ji, Y.; He, W.; Crystal, A.; De Vita, S.; Curigliano,
1429 G. A. Phase I Study of LSZ102, an Oral Selective Estrogen Receptor
1430 Degradar, with or without Ribociclib or Alpelisib, in Patients with
1431 Estrogen Receptor-Positive Breast. *Cancer. Clin Cancer Res.* **2021**, 27
1432 (21), 5760–5770.
- 1433 (65) Tamura, K.; Mukohara, T.; Yonemori, K.; Kawabata, Y.; Nicolas,
1434 X.; Tanaka, T.; Iwata, H. Phase 1 study of oral selective estrogen
1435 receptor degrader (SERD) amcenestrant (SAR439859), in Japanese
1436 women with ER-positive and HER2-negative advanced breast cancer
1437 (AMEERA-2). *Breast Cancer* **2023**, 30, 506–517.
- 1438 (66) Minor, W.; Cymborowski, M.; Otwinowski, Z.; Chruszcz, M.
1439 HKL-3000: the integration of data reduction and structure solution–
1440 from diffraction images to an initial model in minutes. *Acta*
1441 *Crystallographica Section D Structural Biology* **2006**, 62, 859–66.
- 1442 (67) Liebschner, D.; Afonine, P. V.; Baker, M. L.; Bunkóczi, G.; Chen,
1443 V. B.; Croll, T. I.; Hintze, B.; Hung, L. W.; Jain, S.; McCoy, A. J.;
1444 Moriarty, N. W.; Poon, B. K.; Prisant, M. G.; Read, R. J.; Richardson, J.
1445 S.; Richardson, D. C.; Sammito, M. D.; Sobolev, O. V.; Stockwell, D. H.;
1446 Terwilliger, T. C.; Urzhumtsev, A. G.; Videau, L. L.; Williams, C. J.;
1447 Adams, P. D. Macromolecular structure determination using X-rays,
1448 neutrons and electrons: recent developments in Phenix. *Acta*
1449 *Crystallogr. D–Struct. Biol.* **2019**, 75, 861–877.
- 1450 (68) Emsley, P.; Lohkamp, B.; Scott, W. G.; Cowtan, K. Features and
1451 Development of Coot. *Acta Crystallogr. D - Biol. Crystallogr.* **2010**, 66,
1452 486–501.